Annals of Nuclear Energy xxx (xxxx) xxx

Contents lists available at ScienceDirect

Annals of Nuclear Energy

journal homepage: www.elsevier.com/locate/anucene

Coupled system thermal Hydraulics/CFD models: General guidelines and applications to heavy liquid metals

A. Pucciarelli [a,*], A. Toti [b], D. Castelliti [b], F. Belloni [b], K. Van Tichelen [b], M. Moscardini [a], F. Galleni [a], N. Forgione [a]

[a] Dipartimento di Ingegneria Civile e Industriale, Università di Pisa, L.go Lucio Lazzarino n. 2, Pisa, Italy
[b] SCK-CEN, Boeretang 200, 2400 Mol, Belgium

ARTICLE INFO

Article history:
Received 29 May 2020
Received in revised form 2 October 2020
Accepted 29 October 2020
Available online xxxx

Keywords:
Coupling
Guidelines
CFD
STH
Liquid Metals

ABSTRACT

This work aims to review the general guidelines to be adopted to perform coupled System Thermal Hydraulics (STH)/CFD calculations. The coupled analysis is often required when complex phenomena characterized by different characteristic time and length scales are investigated. Indeed, by STH/CFD coupling the main drawbacks of both stand-alone codes are overcome, reducing the computational cost and providing more realistic solutions. A review of several works available in literature and involving different coupling approaches, codes, time-advancing schemes and application fields is given. Besides STH/CFD coupling techniques, spatial domains and numerical schemes are analysed in detail. A brief description of applications to heavy liquid metal systems is also reported; lessons drawn in the frame of these and other works are then considered in order to develop a set of good practice guidelines for coupled STH/CFD applications.

1. Introduction

The simulation of phenomena involving very different characteristic time and length scales is a common issue in several application fields; these scales can span between the micro-scales of turbulence, neutron kinetics and molecular diffusion to the large ones associated to the overall behaviour of the whole system. Currently, no stand-alone code seems able to provide reliable predictions of large systems allowing both a good accuracy for regions involving complex flow behaviours on small time scales and an affordable computational cost; consequently, these phenomena need to be investigated with dedicated models.

System Thermal-Hydraulics (STH) codes are widely adopted for the evaluation and prediction of phenomena that may occur in large systems and proved interesting capabilities in different applications also thanks to their versatility. Nevertheless, because of the adopted 1D approach, they are not fully reliable for the simulations of situations which are intrinsically multi-dimensional like, for instance, those involving heat and mass transfer inside pools and boilers.

On the other hand, CFD tools may provide noteworthy capabilities in simulating complex 3D phenomena; however, they might require very large computational efforts to simulate transient phenomena. In addition, in particular applications, such as the ones in the nuclear field, CFD tools are not as flexible as STH codes for simulations involving neutron kinetics and control systems, so extra time has to be allocated to converge to a stable CFD model, reproducing correctly the functioning of the facility.

In this framework, the use of coupled STH/CFD calculations may overcome the limits reported by each stand-alone approach thus providing the capability of exploiting the positive features of both CFD and STH codes. Preliminary coupled simulations can even be used in support of the development of less computational-cost CFD model, depending on the type of considered transient and associated relevant phenomena.

1.1. General related works

During the last years, numerous authors working in different application fields provided valuable contributions in support of the development of good practices to be established for the code to code coupling. Several coupling approaches involving different codes, time-advancing schemes and STH/CFD information exchange interfaces were investigated, generating a sound background for drawing the learned lessons and proposing a series of general guidelines.

* Corresponding author.
E-mail address: andrea.pucciarelli@dici.unipi.it (A. Pucciarelli).

https://doi.org/10.1016/j.anucene.2020.107990
0306-4549/

Nomenclature

Symbols

h	Convective heat transfer coefficient
$\dot{m}$	Mass flow rate
P	Pressure
q''	heat flux
R	Residual vector
S	Source term
t	Time
T	Temperature
U	Input vector
Y	Output vector
ΔP	Pressure drop
ε	Threshold value for convergence criteria
Φ	Operator transforming U in Y
ω	Relaxation factor

Superscripts

k	Current internal iteration
n	Current time step

Subscripts

f	averaged in the fluid volume, i.e Bulk
M	Momentum
T	Thermal
w	Wall

Acronyms

ACS	Above Core Structure
CFD	Computational Fluid Dynamics
FPS	Fuel Pin Simulator
LMFBR	Liquid Metal Fast Breeder Reactor
LOF	Loss Of Flow
MYRRHA	Multi-purpose hYbrid Research Reactor for High-tech Applications
LOF	Protected Loss Of Flow Accident
SG	Steam Generator
STH	System Thermal Hydraulics

More specifically, in the works of Aumiller et al. (2000, 2001) coupling techniques between the RELAP5-3D (INL, 2005)STH code and the ANSYS-CFX CFD (ANSYS Inc., 2013) code were tested using both explicit and implicit coupling schemes and an increase of the calculation stability was observed when adopting the implicit approach. In recent times, the work by Bertolotto et al. (2009) showed the superiority of coupled STH/CFD approaches in describing 3D environments in comparison to 1D STH stand-alone calculations; in particular, TRACE (US NRC, 2007) STH code and ANSYS-CFX CFD code were considered and applied to a double T-junction case. In later studies, coupling applications involving RELAP5 and ANSYS-Fluent (Li et al., 2014) and STAR-CCM+ and TRACE (Grunloh and Manera, 2016; CD-adapco, 2012) were performed, also highlighting the impact of the selected spatial discretization techniques (overlapping or non-overlapping) on the capabilities of the considered coupled code application.

Concerning the application fields, coupled calculations were successfully adopted for the simulation of boilers furnaces and steam generators of coal-fired and combined heat and power plants. Park et al. (2010) presented a coupled model to simulate a part of the Youngheung coal combustion power plant aiming at investigating relevant involved phenomena and to estimate important parameters. ANSYS-CFX was used to carry on the 3D CFD analysis of the furnace, while PROATES Off-Line (E.ON Engineering, 2007) to model the 1D boiler. The models are coupled by exchanging temperature and heat flux values on the furnace walls and heat exchangers at each iteration of the coupled calculation.

In (Schuhbauer et al., 2014) Schuhbauer et al. presented a detailed boiler simulation obtained by interfacing the fire with the steam side by means of a dedicated coupling algorithm. The steam side was simulated by the commercial software package APROS (APROS, 2012), while adjusted ANSYS-FLUENT (ANSYS Inc., 2013) models were used to simulate pulverized coal combustion. The code to code interfacing was assured by a MATLAB routine. The information exchange between the codes occurred through an iterative process: the heat flow is exported from ANSYS and is applied as boundary condition in APROS simulation; the inner wall temperature is then calculated in APROS and imported in ANSYS.

A novel integrated model of a steam drum and circulation system in a coal-fired boiler was proposed by Edge et al. in (Edge, 2011). Here, the heat input was calculated by using a CFD model instead of being approximated as a total heat duty, while by using gPROMS 3.2 (Enterprise, 2009) the 1D process model for steam generation in natural circulation boiler is created. The heat flux values were obtained with the CFD analysis, they were subsequently regressed into a function of height and used to drive the process model.

Hovi et al. in (Hovi, 2017) presented an integrated transient approach for simulating a Bubbling Fluidized Bed (BFB) boiler furnace coupled to the steam cycle. The BFB furnace was simulated with an in-house CFD model implemented in ANSYS-FLUENT (ANSYS Inc., 2013) while the steam cycle was simulated with the dynamic process solution software APROS (APROS, 2012). A two-way coupling was established by transferring the heat flux evaluated by the CFD analysis to APROS and the wall temperature obtained with APROS back again to ANSYS.

Other possible applications involve the use of coupled codes in order to obtain better estimations of the physical and thermodynamic properties of the involved materials. A method connecting CFD simulators to the code ASPEN Plus (AspenTech, 2014) aiming for an improvement of the thermodynamic modelling in computational fluid dynamic simulations was presented in (Vaquerizo and Cocero, 2018) by Vaquerizo and Cocero. Here, the code ASPEN Plus instantaneously calculates and provides any physical property required for the simulation to the CFD analysis tool. The connection is created via MATLAB (MATLAB., 2018) and Excel-VBA.

1.2. Works related to liquid metals Fast reactors (LMFR)

Moving to applications specifically developed for liquid metals, several works reported in literature mainly refer to lead and sodium cooled reactors for nuclear applications. Liquid Metal cooled Fast Reactors (LMFRs) represent one of the most valuable perspectives for the development of Generation IV Nuclear Power Plants. Examples of their application to power generation proved promising capabilities and provided interesting material for further developments. In this sense, the french Super-Phénix and the russian BN-600 represent important applications and confirmations of the feasibility of LMFRs, thus paving the way for the development of new reactor concepts. A step forward in the development of LMFRs is represented by the MYRRHA Accelerator-Driven System (De Bruyn et al., 2015), which aims at decreasing the amount of nuclear waste to be relocated in geological disposals

while improving safety features. The use of passive cooling systems based on natural circulation heat transfer mechanisms represents both a fundamental feature and a challenging task for the development of these reactors, requiring the use of different tools for a deep and precise understanding of the involved phenomena. In addition, these phenomena may act on time-scales and length-scales which cannot be reliably managed by a single approach, thus requiring multi-scale and multi-physics techniques. Furthermore, unlike typical LWRs, several plant components cannot be reliably modelled using a 1D approach, since the proposed LMFR designs usually feature large 3D environments, such as the reactor pool. As a consequence, stand-alone STH calculations are no more suitable for the creation of a well posed problem and a qualified nodalization. On the other hand, CFD codes can predict flow conditions in 3D environments but require large computational costs. In this sense, the development of coupled STH/CFD calculations aims at providing a tool that could suitably reproduce the addressed plant operating and accidental conditions. In such applications, CFD would be essentially involved for the large 3D environments, such as the reactor pool, while STH codes would keep modelling all the other components of the plant, such as the primary pumps, the core and the heat exchangers. The following application examples demonstrate that the scientific community is very active in the development of coupled modelling techniques in support of the design of Generation IV LMFRs. The present paper, proposing general guidelines for the creation of qualified STH/CFD applications, specifically aims at paving the way for the recognition of CFD tools, and STH/CFD applications in particular, as suitable tools for the design and licensing of Nuclear Power Plants (NPPs).

At SCK•CEN, (Toti et al., 2017a, 2017b) developed a multi scale system thermal hydraulic CFD coupling methodology for high-fidelity integral system simulations. The combined use of the CFD code ANSYS-FLUENT and the system code RELAP5-3D was applied to model the experimental facility E-SCAPE (Van Tichelen et al., 2015), a scale mock-up of MYRRHA reactor, and to simulate a postulated Loss Of Flow (LOF) accidental condition. Several coupling schemes were tested and compared in terms of robustness, convergence rates and computational effort. The modelling capability of the coupled system and its applications was then extended in (Toti et al., 2018a, 2018b).

Further works performed at the Belgian Nuclear Research Centre (SCK•CEN) (Toti et al., 2017a, 2018b, 2018c; Van Tichelen et al., 2015; Toti, 2018), University of Pisa (Martelli, 2015; Angelucci, 2018; Angelucci et al., 2017; Forgione et al., 2019; Martelli et al., 2017, 2014; Pucciarelli et al., 2020) and at the Royal Institute of Technology (KTH) (Jeltsov et al., 2013) must be taken into account. In particular, at the University of Pisa a coupling methodology involving the modified version of RELAP5/Mod3.3 (Barone et al., 2019) STH code and the ANSYS-Fluent CFD code was developed, aiming at performing calculations reproducing the experimental results obtained both from closed loop (NACIE-UP (Di Piazza et al., 2013) and pool type (CIRCE (Pesetti et al., 2018) facilities. Different approaches involving both explicit and semi-implicit coupling schemes were considered, and both forced and natural circulation tests were performed obtaining promising results.

At KTH calculations were performed trying to reproduce experimental data from the TALL-3D facility (Grishchenko et al., 2015) consisting in a loop also containing a component where 3D effects are supposed to be relevant. The selected codes were RELAP5/Mod3.3 and STAR-CCM+: the results highlighted relevant feedbacks between the 3D phenomena occurring in the dedicated 3D component and 1D loop behaviour also providing a better prediction of the considered experimental data.

Concerning multi-code (more than two) coupling, the work performed at CEA by Gerschenfeld et al. (Gerschenfeld et al., 2017) must be also highlighted: in order to suitably simulate relevant different characteristic scales, they combined the capabilities of the STH code CATHARE3 (Baviere, 2012), of the sub-channel code TrioMC (Conti, et al., 2015) and of the CFD code TrioCFD (Barthel, 2012). The work main outcome is the integrated code MATHYS (Multiscale ASTRID Thermal-HYdraulics Simulation), which proved promising capabilities and granted feedbacks exchange between the three involved codes.

For general information about coupling techniques applied to LMFRs the reader is also referred to (Roelefs, 2019).

1.3. Scope of the work

In this work a survey of the methodologies reported in literature concerning the CFD/STH coupling is presented. Among the mentioned application fields, the literature review of the application examples is mainly focused on heavy liquid metals, proposing some good practice guidelines for the modelling of multi-scale multi-physics phenomena through coupled codes. In Section 2 coupling techniques are defined and classified, Section 3 describes the spatial domains while Section 4 investigates the numerical schemes. Section 5 gives some application examples on heavy liquid metals, while conclusions are reported in Section 6.

2. Definitions and classification of code coupling techniques

In the available literature, several code coupling techniques exist. For the sake of clarity, before proposing practice guidelines, it is worth providing definitions and classification of these techniques.

As reported by (Mengali et al., 2012), a coupled system is the result of the interaction of two or more sub-systems. These sub-systems, each one presenting its own set of governing equations, share some of the variables needed for the resolution of its own set of differential equations; consequently, none of these sets can be solved without receiving information from the others.

According to (Toti, 2018), the coupling techniques may be classified taking into account six different characteristics:

- Code Integration
- Coupling Execution
- Synchronisation
- Information Exchange Type
- Spatial Domains
- Numerical Scheme

The presently considered classification is not the only one proposed in literature. Different characteristics were identified in other works (see e.g. Zhang, 2020) suggesting that the nomenclature and definitions in the code coupling environment are still evolving and debate is open.

In similarity with other works (Zhang, 2020), we can also identify several classification groups, or levels, to which these characteristics belong. In the present work, three main levels are considered: the architecture level, the operative level and the numerical level. The architecture level defines the structure of the considered coupling approach, specifying if a single multi-physics code or different specialized codes shall be adopted. At the operative level, instead, the way the codes work and share information is defined, also stating the coupling execution and the synchronisation issues. Eventually, at the numerical level, the spatial domain subdivision and the adopted numerical schemes for the temporal discretization are selected. In the following, each characteristic is described showing the possible choices that could be made in the path for the creation of coupled STH/CFD application.

2.1. Code integration

When considering Code Integration (System Architecture Level), the coupling techniques may be subdivided into two main different groups: Monolithic and Partitioned Solutions.

In the former case a single code is developed for the solution of all the sub-systems; depending on the addressed domain the solver adopts different solving strategies. The main advantage of this approach is that good performances may be achieved for very specific problems with tuning and optimization processes. On the other hand, highly specialized algorithms may not be ductile and suitable for a wide range of operating conditions. In addition, to the authors' best knowledge, at least for thermal-hydraulics phenomena investigations, this approach cannot rely on existing codes, thus requiring further development, verification and validation processes. Monolithic approaches are instead often adopted for fluid-structure interaction problems (see e.g. Aulisa et al., 2018) and (Langer and Yang, 2018), such approach is also available in the commercial code ANSYS Workbench.

A Partitioned approach, instead, adopts a dedicated solver for each of the sub-systems or physical phenomena; a master code, or interface software, provides the communication between the adopted codes. This is the most common approach adopted in the available literature since it is the simplest to implement and does not require access to the source codes. In addition, an increasing number of commercial codes, both STH and CFD, is now equipped with a dedicated code coupling interface software, which provides further support for the development of coupled applications. A possible downside of this approach is the information transfer system that, in some cases, may require a significant computational time. On the other hand, the user may select the codes that could fit best for the modelling of each region and phenomenon, allowing for further flexibility of the approach, which requires work only at the interface code level, without involving changes in the main structure of the computational codes (see e.g. Schuhbauer et al., 2014; Toti et al., 2017).

2.2. Coupling Execution

At the Operative Level Off-line and In-line approaches may be adopted when considering Coupling Execution.

An Off-line approach defines a weak connection between the domains of the coupled codes; each code provides the other with updated boundary conditions and only one-way feedbacks exist between the codes (see e.g. Martelli et al., 2017; Galleni et al., 2020). As an example, when considering fluid–solid interactions, possible structure displacement due to thermal stresses or turbulence induced oscillations may impact on the fluid flow and turbulence structures themselves thus implying mutual feedbacks between the two codes. With an Off-line approach, these phenomena cannot be fully observed and only one-way effects can be investigated (e.g. the effect of fluid flow on structures, but not viceversa).

An In-line approach instead provides the user with the capability of observing mutual influencing phenomena between the addressed domains (see e.g. Aulisa et al., 2018; Langer and Yang, 2018), thus implying a two-ways feedback; nevertheless, additional efforts are required in order to improve the connecting and information transferring capabilities of the considered coupling interface, since it might require a more precise synchronisation algorithm. This is the most common approach in STH/CFD coupling techniques and it was also adopted in all the application examples reported in Section 5. In case a monolithic approach is selected at the code architecture level, this approach is strongly recommended. In fact, since the Monolithic approach aims at creating a highly specialized code, not considering possible two-way effects between the various sub-systems, as happens in the Off-line approach, would not be cost effective.

Because of their characteristics, the Off-line and In-line approaches are often termed also as One-way and Two-way coupling respectively.

2.3. Synchronisation

Synchronisation concerns the approach adopted by the codes for the definition of the temporal coordinates at which the information transfer occurs. Identical Time steps or Sub-cycling approaches may be in general adopted. This characteristic again belongs to the Operative Level. Since for the Monolithic code integration solution a single multi-physics code exists, the Identical Time steps approach is recommended. With a Partitioned code integration instead, which is more ductile, the user can opt for both the synchronisation approaches.

In case of the Identical Time step approach is selected, all the adopted codes use the same time-step; synchronisation consequently occurs at the end of each time-step. The time-step size may be defined externally via a code-interface software or could be adaptively defined by one of the codes, according to its own convergence or stability requirements. The first approach allows a parallel running of the solving codes, the latter requires instead the "slave" code to wait for the "master" code concluding its own calculation for the definition of the next time step at which synchronisation occurs.

When adopting a Sub-cycling approach instead, codes use different time-step and data transfer is performed at some synchronisation points only (see e.g. Toti et al., 2018; Galleni et al., 2020). This technique allows each code working in its optimal conditions, choosing the most suitable time-step size for the simulations of its corresponding domain. In particular, it could be a valuable approach when addressing physical phenomena or sub-systems presenting relevantly different characteristic time scales. On the other hand, in order to assure a correct coupling, the user must be sure that both codes reach exactly each synchronisation point in order to avoid possible stability or accuracy issues.

Concerning examples of coupled STH/CFD applications available in literature, the adopted approach often involves a "macro" time-step on the CFD side while STH code solves the same time interval adopting smaller time-steps. This approach allows the two codes working in a suitable manner and, contemporary, limiting the number of time steps on CFD side, thus considerably reducing the total computational effort. This approach was in example adopted in (Di Piazza et al., 2013).

2.4. Information exchange type

When considering this characteristic, again belonging to the operative level, coupling approaches may be subdivided into two groups: Sequential and Parallel coupling.

Sequential coupling occurs when, while one code is running, the other ones are waiting, idle, for the end of the present time-step calculation. Once the first code ends its run, it provides the other codes with the relevant updated information needed for performing each separate calculation. This is the most common approach in STH/CFD coupling techniques and it was also adopted in all the application examples reported in Section 5.

A Parallel Coupling approach, instead, requires all the codes to run simultaneously. This solution could be really valuable when working with calculations requiring similar computational times since it could contribute in reducing the dead times; on the other hand, it requires caution in the information transfer phase since, lacking mutual feedbacks between synchronisation points, it may cause numerical instabilities.

Consequently, when working with codes that usually require different computational times, which is the case of CFD and STH codes, a Sequential Coupling approach is suggested. In case a Monolithic approach is considered at the architecture level, the parallel coupling approach is recommended. In fact, running all the sub-codes in parallel would allow the simultaneous resolution of the considered transport equations, thus improving the stability of the problem.

2.5. Spatial domain

At the Numerical level, the considered spatial domains may be overlapping or non-overlapping.

In the former case, superimposed domains are considered. A code performs calculations resulting in the definition of source/sink terms in the governing equations of the others, so that a continuous domain may be obtained. As an example, a STH code may be adopted to simulate the behaviour of a complex system, whilst the CFD code is used instead only for the calculations of the regions in which 3D effects are worthwhile to be investigated. The information provided by the CFD code is used to refine the parameter settings of the STH code for those environments in order to reproduce, with higher accuracy, phenomena that could not be predicted by a 1D code running in stand-alone.

When adopting a non-overlapping approach (from here on termed as the Decomposition approach), no superimposition between the spatial domains of the codes occurs; each code solves the assigned domain and provides updated boundary conditions to the others at each synchronisation point. None of the codes consequently works in a continuous domain. As an example, while the global system may be simulated by a STH code, some regions, involving flow fields where 3D effects are relevant, are missing from the STH domain and are instead replaced by a domain simulated by, e.g., a CFD code. The STH and CFD codes exchange information at each synchronisation and mutually provide updated boundary conditions. Further information is provided in section 3.

2.6. Numerical scheme

Decisions about the time-discretization are again performed at the numerical level. Concerning the numerical scheme for data transfer, the coupling approaches may be subdivided into three main families: the explicit, the semi-implicit and the fully implicit ones.

When adopting an explicit approach for data exchange, serial calculations are performed, with no actual check on the results provided by the codes. Each code indeed runs a one-through calculation; its results are used as new boundary condition for the other code, and vice versa, without any kind of control before proceeding to the next synchronisation point. The implementation of this scheme is relatively easy, nevertheless it requires further analyses concerning the adopted time step. If the time step is not sufficiently small, the obtained prediction may be affected by dangerous oscillatory behaviours, which may also imply instabilities (see e.g. Martelli, 2015) as application example).

Semi-Implicit approaches instead require iterative calculations before proceeding to the next synchronisation point. The results provided by each code are again used as updated boundary condition for the other but, before proceeding to the next synchronisation point, the coupling scheme evaluates the consistency of the obtained results at the interfaces between the two codes. If the obtained results are sufficiently close (acceptance criterion defined by the user), the scheme proceeds to the next time-step, while in case the convergence condition is not respected, another internal iteration is performed and calculations for the same time-step are repeated with updated boundary conditions. This approach should grant higher robustness to the coupling scheme, allowing the user to adopt larger time-step without occurring in instabilities (see e.g. Toti et al., 2018a, 2018b) as application examples).

Fully implicit approaches, instead, require the simultaneous resolution of all the considered transport equations. The obtained coupling is very strong, and it is enforced at every time step and internal iteration. They can only be adopted if the monolithic approach is selected at the code architecture level. This approach can be hardly considered if a partitioned integration is instead adopted since it is practically impossible to simultaneously solve all the equation sets when dealing with two (or more) commercial codes.

The presently adopted definitions of "explicit" and "implicit" must not be confused with the ones commonly used for the solving schemes for Partial Differential Equations. These definitions only refer to the scheme ruling the data transfer between the considered codes and cannot be used as means for aprioristic definitions of the stability boundaries of the scheme, which is not in general assured even for the "implicit" approach (Toti, 2018).

Further information on the coupling explicit and semi-implicit schemes commonly adopted in literature is reported in section 4. Fully implicit schemes are instead not reported because the resolution schemes available in literature for classical thermal-hydraulics problems may be also adopted. In addition, being practically applicable to Monolithic approaches only, fully implicit schemes may be strongly dependent on the considered problem, thus being unsuitable for a more general description, which is the aim of the present work.

2.7. Further considerations

In the present Section 2, a possible classification of the coupling approaches is exposed, trying to present the various characteristics and briefly describing their impact on the code to be developed and on the expected model stability. Fig. 1 resumes all the presented characteristics and their subdivision among the three levels.

Depending on the selected application, some approaches may result more suitable than others.

For example, when firstly approaching a new thermal–hydraulic problem (e.g. a new experimental facility), the initial steps towards the application of code coupling should involve a ductile coupled approach. A Partitioned, Off-Line, Sequential coupling considering the Decomposition approach and an Explicit time discretization may be particularly suitable. In fact, it would be appliable in a wide range of operating conditions and would allow changes to its structure (e.g. selecting different spatial decompositions) without requiring impactful modifications to the source codes. On the other hand, it would enforce a weak coupling, which may not consider all the possible involved phenomena, thus limiting the quality of the obtained results; in addition, the computational efficiency of the so-developed model could be limited.

On the contrary, in front of a well-defined problem which is not going to undergo relevant changes (e.g. a licensed nuclear loop), the most highly specialized approach could be, instead, the best option in order to obtain a more refined coupling scheme. The user may consequently choose a Monolithic, In-Line, Parallel coupling considering Identical time steps. The Overlapping approach and a Fully implicit numerical scheme may also be considered in order to tighten the coupling bond. On the other hand, these advantages require the development of a dedicated software which, up to date, cannot rely on commercial codes; the introduction of new models and schemes may also require relevant amount of work.

As a consequence, there is no pre-defined recipe to be followed and the user must decide which option best fits the problem, trying to find the best compromise between the positive and negative aspects of each modelling technique.

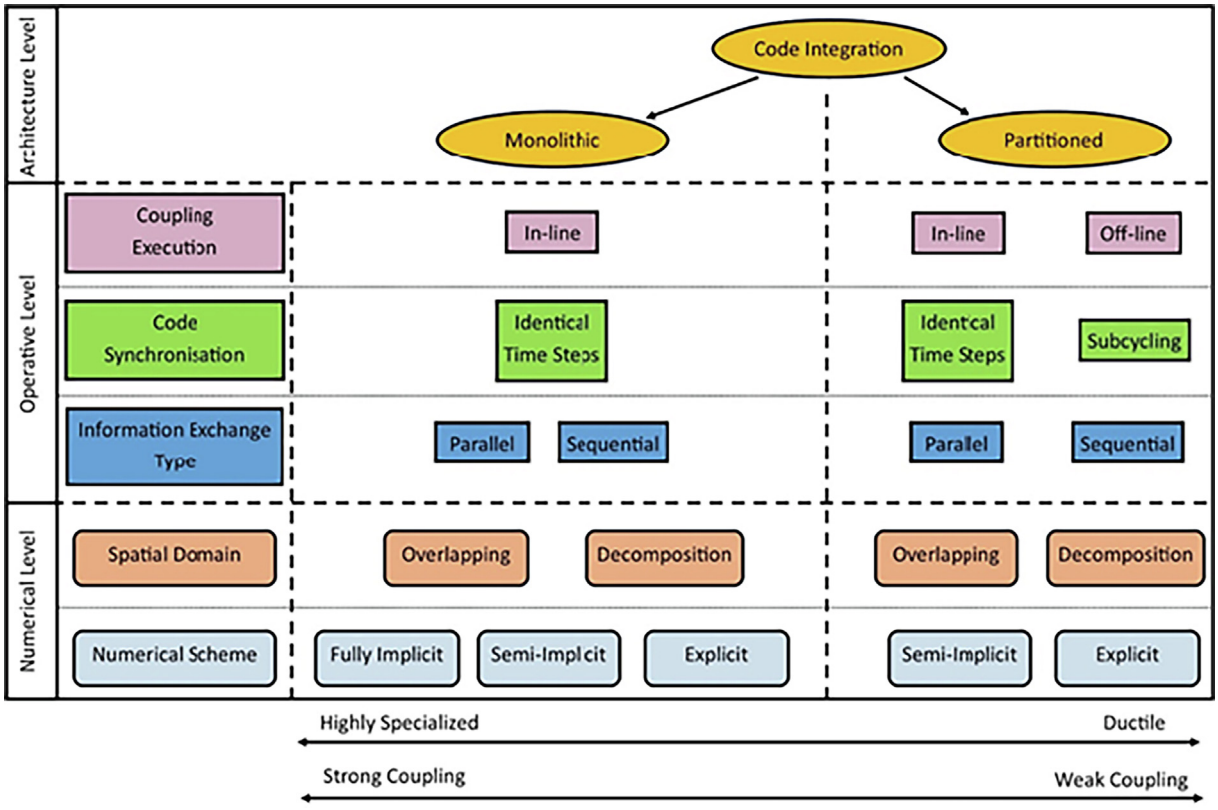

Fig. 1. Code coupling classification.

3. Spatial domains approaches: a deeper insight

As anticipated in the previous section, the definition of suitable spatial domains is a relevant phase in the development of a multi-scale coupled code. In the present section, the typical adopted coupling schemes for thermal–hydraulic boundaries are further described. The main information sources for this section may be found in (Toti, 2018; Roelefs, 2019).

As a general good practice, the boundaries between STH and CFD domains should be carefully defined: regions in which no complex phenomena occur, e.g. far from recirculation zones, should be selected, in order to avoid undesired effects during the information transfer phase. Furthermore, it should always be considered that each information transferred between such different codes always implies some assumptions to be performed for its implementation and information loss. In general, during information transfer from CFD to STH codes, data averaging or integration processes are performed; information about the velocity and temperature profiles is consequently lost. On the other hand, interpolations or distribution assumptions may be required for data transfer in the other direction. It is consequently clear that, in regions where the involved phenomena are not sufficiently linear, suitable averaging and interpolation processes could unlikely be found or considered totally reliable.

After having assigned each region to the proper simulation technique and having paid attention to the boundaries positioning, the subsequent decision regards the technique to be used for the interaction between the spatial. As anticipated in section 2.5, the main choice is between overlapping and decomposition approaches. Fig. 2 shows the concept at the basis of each approach; filled circles represent the centres of STH domain control volumes, while empty circles represent instead the junctions (between control volumes or towards boundaries).

As discussed in Section 2.5, in the overlapping approach, the whole system is assigned to a single code, while other codes are adopted for the sake of performing refined calculations in some selected regions; the CFD and STH domains are superimposed and both perform simulations on the common regions. In this way the main code, usually the STH one, may also run calculations in stand-alone without any further significant change to its domain structure; the CFD code instead supports its calculation providing suitable coefficients tunings in the regions selected for refined calculation. The outcome is a STH code which behaves coherently

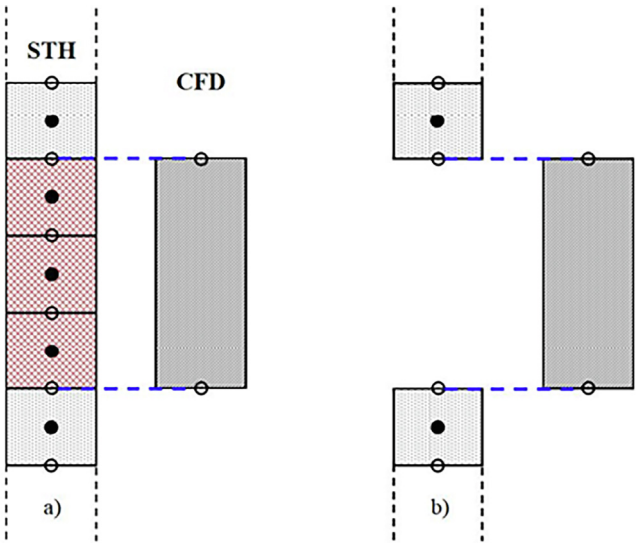

Fig. 2. Concepts of Overlapping (a) and Decomposition (b) approaches.

with CFD predictions in the overlapped regions; checks assuring matching between temperature, pressure and mass flow variations at the boundaries of the overlapped regions are performed.

When adopting a decomposition approach, instead, none of the codes models features a domain structure that could be adopted in stand-alone calculations as it is. In fact, the domain is divided into two or more parts, each one being assigned to a dedicated solving technique. No spatial overlapping usually occurs, though, sometimes, partial superimpositions may be introduced.

In the following, the typical adopted coupling schemes for thermal–hydraulic and thermal boundary interfaces are described, also highlighting the capabilities and downsides of each coupling approach.

3.1. Thermal-Hydraulic boundaries

Fig. 3 shows the general transfer data schemes to be adopted when considering decomposition and overlapping approaches for thermal–hydraulic boundaries. Filled and empty circles maintain the same meaning of Fig. 2; red connectors represent transfer data from STH to CFD, while the blue ones represent instead transfers from the CFD to the STH code. Solid lines refer to imposed conditions, while the dashed ones instead represent checks to be fulfilled before proceeding to the next time step. It is here remarked that, as shown in Fig. 3, though STH codes provide the user with pressure values calculated at centre of each node, the pressure value to be exchanged with the CFD code is the one at the interface. If not directly made available by the code, the user must calculate this value, e.g. via a linear extrapolation or approximations which better fits the considered application.

The most important task for both approaches is granting consistency for the information transfer between STH and CFD codes and vice versa; this means that mass, energy and momentum balances must be respected at the boundary interfaces.

3.2. Overlapping approach

As shown in Fig. 3 (a), when dealing with an overlapping approach, several coupling operations must be performed: these include imposing suitable boundary conditions at the interfaces and checking the consistency of relevant quantities in some of the STH volumes.

At the boundary interfaces the temperature information from the STH calculation is imposed for the CFD domain. This provides the CFD domain with the required temperature information concerning inlet temperatures, regardless of the flow direction (Fig. 3 suggests an upward flow direction, however the method is generalisable for every flow direction).

Information regarding the mass flow rate is also required by the CFD code. The most common approach reckons on the definition of a mass flow rate at one of the ends of the CFD domain, adopting instead an imposed constant pressure value at the other end. This choice is usually recommended even in CFD stand-alone applications, since it grants higher calculation stability providing the code with suitable boundary conditions and a well posed problem.

The CFD code, on the other hand, must provide the STH code with suitable coefficients corrections or source terms: these may include, depending on the addressed conditions, distributed or local pressure drop coefficients and energy and/or momentum sources. This allows the STH code producing results that it would never provide in stand-alone applications because of its intrinsic limitations, such as the inability to reliably predict 3D phenomena or particular flow conditions. For example, a fixed local pressure drop coefficient proved not to be suitable for a STH stand-alone calculation; with a coupled STH/CFD approach, the CFD calculation may provide a good estimation of the needed pressure drop coefficient depending on the actual flow conditions (Reynolds number), thus improving the pressure distribution prediction in the whole system. Another possible application could be the introduction of energy source terms (S_T in Fig. 2), in order to better reproduce a

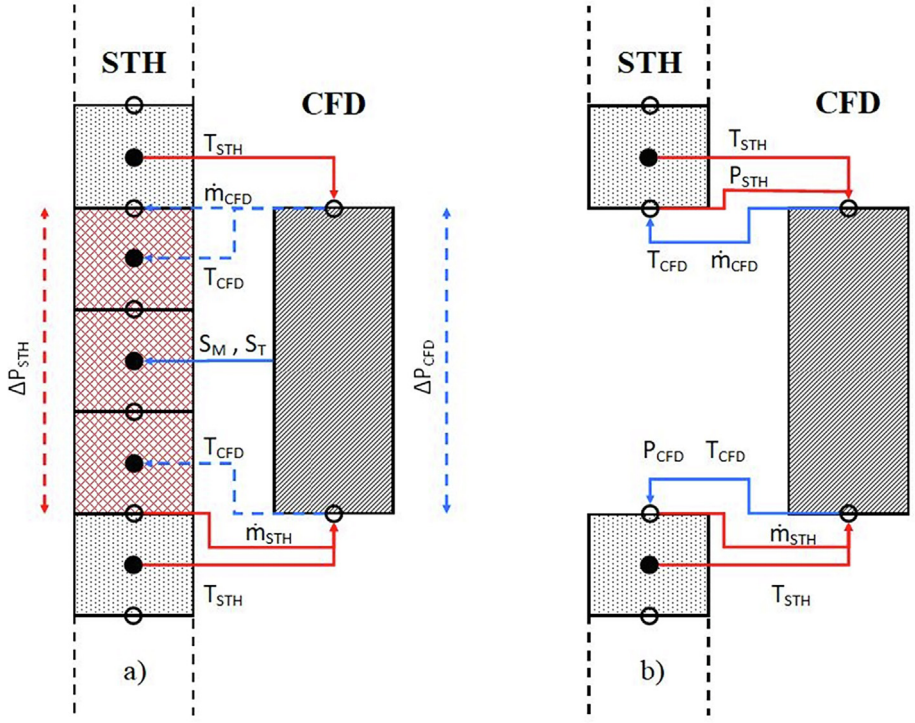

Fig. 3. Schemes for Overlapping (a) and Decomposition (b) approaches for Thermal-Hydraulic boundaries.

given temperature trend, e.g. due to recirculation phenomena occurring in the CFD domain.

In order to grant consistency between the STH and CFD calculations, several checks must be performed. In particular, mass flow rates at the location corresponding to the CFD pressure outlet section are compared and the pressure drops in the two domains are evaluated. Temperature is instead evaluated at the centre of the volumes next to the interface, following the commonly adopted staggered mesh approach. By performing iterative tunings of the source terms appearing in the STH momentum and energy equations, e.g. S_M and S_T in Fig. 3(a), it is possible to reach a good match between the predictions of the coupled codes. Source terms may be distributed in all the STH side volumes or concentrated in just one location: it is up to the user deciding the adopted discretization refinement. It is clear that obtaining a perfect balance is practically impossible, therefore the user has to define the tolerance to be adopted for the convergence condition for each quantity.

3.3. Decomposition (Non-Overlapping) approach

The Decomposition approach subdivides the global domain into several domains, each one addressed by a single code. As Fig. 3(b) clearly shows, this technique requires a simpler connection scheme between the coupled codes: information transfer occurs only at the interfaces without involving other regions.

Input mass flow and temperature information at the interfaces are again required by the CFD code as it happens for the overlapping approach; information regarding the pressure value to be imposed is required at the pressure boundary as well. This last information is needed since the pressure is now one of the relevant quantities that the CFD domain must provide the STH code with, together with mass flow and temperature information. By imposing all the relevant quantities at the interfaces, the energy, mass and momentum balances are granted, thus implying a tighter and more conservative coupling.

However, imposing a variable pressure at one of the CFD domains boundaries generally implies that a completely new pressure field must be calculated at every iteration. This may increase the computational effort and, sometimes, it may create stability issues. A possible solution may be obtained considering a slightly different coupling scheme and maintaining instead a constant relative pressure value (e.g 0 Pa) for the Pressure Outlet surface of the CFD domain. This approach would reduce, yet not obviously making disappear, the changes affecting the pressure fields at every iteration; the new information to be provided to the STH code becomes the pressure drop across the CFD domain.

Fig. 4 reports a scheme of the presently considered approach. As it can be observed, no pressure information is now provided to the CFD code. The CFD code provides the pressure drop between the ends of its domain; a new pressure value is calculated and then provided to the STH code using the following relation

$$P_{CFD} = P_{STH} + \Delta P_{CFD} \quad (1)$$

It is worth mentioning that the ΔP_{CFD} must take into account the hydraulic head connected to the height of the CFD domain, which has to be the same of the STH components replaced by the CFD non overlapping region.

For pool type facilities, see e.g. Fig. 5, another type of coupling scheme can be applied (APROS, 2012). If a pool region with a free surface is modelled with the CFD code, it is possible to impose all mass flow rate conditions at the inlet and outlet interfaces of the CFD domain. The convergence is ensured by the feedback on the pressure field that occurs in case of changes in the free surface level in the pool.

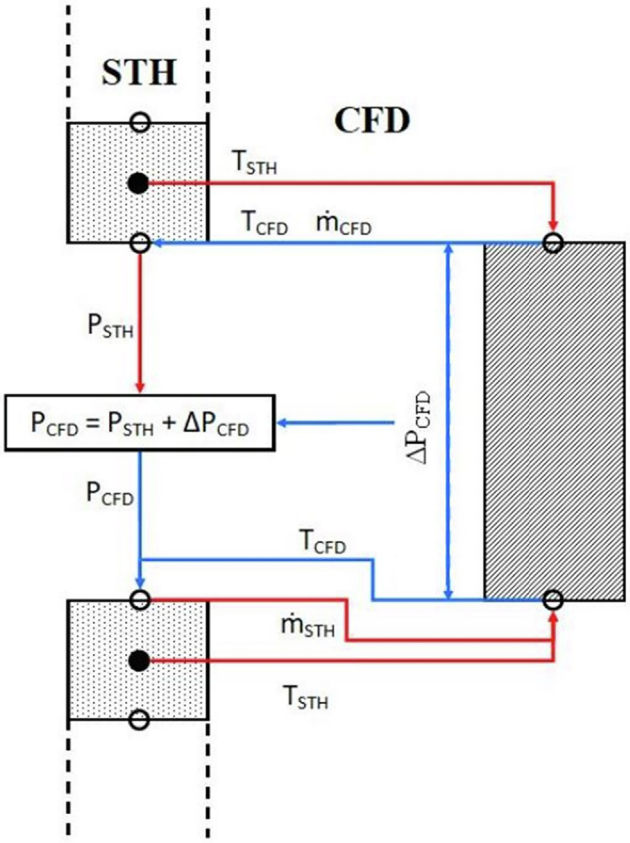

Fig. 4. Decomposition scheme, additional coupling solution.

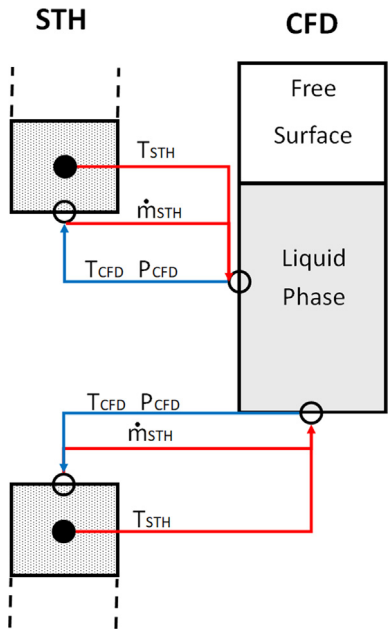

Fig. 5. Decomposition scheme – alternative BC exchange for pool layout.

3.4. Further guidelines for Thermal-Hydraulic boundary conditions

Some general recommendations, common to both spatial schemes, may be provided.

- Balances of mass and energy shall be as far as possible fulfilled in coupled applications since unbalances, in both directions, may imply serious problems for the performed calculations.

As a consequence, the user must especially check the consistency of the thermo-physical properties considered by the adopted codes.

- Concerning the CFD Inlet boundary conditions, in the previous sections the descriptions of the spatial schemes were performed assuming to impose of a mass flow rate because it assures, automatically, the fulfilment of the mass balance. Nevertheless, the user may obviously make different choices.

One may decide to impose a velocity at the boundary interfaces - which for incompressible flows may be considered equivalent to the mass flow condition - once provided that the same flow section and fluid density are maintained across the coupling interface. However, even small discrepancies in the calculation of flow sections and fluid properties, which are performed by different codes, may imply relevant error propagation in the balance terms. On the other hand, one of the advantages of imposing velocity at CFD inlet is the possibility of providing the code with an arbitrary profile, while a mass flow rate condition implies a uniform velocity distribution. As an example, the user may impose a plausible velocity profile for the addressed flow condition; this may lead to improved results by avoiding undesired development length effects. This approach, however, is strongly case sensitive, thus creating a highly specialized approach that could not be suitable for even slightly different flow conditions.

A similar result may be obtained also considering larger CFD domains including regions upstream the coupling interfaces slightly superimposed to the STH domain. This way, a sufficiently long development/discharge length may be simulated, thus providing the region of the non-overlapped domain with improved inlet velocity profiles. The upstream region is usually excluded from the coupled calculation but, if included, it may provide improved results: the computational cost increase of this approach must be however taken into account.

A further possibility involves the imposition of a pressure inlet condition at the STH/CFD interface. The pressure inlet condition again represents a less conservative approach than the one considering an imposed mass flow rate though, for incompressible fluids, they may again be considered equivalent. Nevertheless, by imposing the inlet pressure, no binding is imposed on the inlet velocity profile, which is free to fluctuate. This may imply the prediction of unreliable inlet velocity profiles that may relevantly impair the quality of the performed calculations.

As a consequence, except for cases in which imposing velocity or pressure inlet represent the only viable choice, e.g. when the inlet velocity profile may have relevant impact on the observed phenomenon, selecting a mass flow rate boundary condition is recommended for the sake of obtaining a better calculation accuracy.

3.5. Thermal coupling boundary conditions

Compared to Thermal-hydraulics boundaries, the Thermal ones require less effort for achieving a good coupling in terms of data transfer since only the energy balance across the wall is involved. Nevertheless, several techniques have been proposed in literature, each one showing good capabilities and downsides. In addition, the user must be aware that the CFD domain may require a suitable division in as many subdomains as the STH code control volumes. In particular, volume averaged and surface integral calculations have to be performed when transferring data from CFD to STH, while interpolations processes are instead required in the other direction.

3.6. Overlapping approach

Fig. 6 shows a possible scheme for the thermal coupling when considering the Overlapping approach. In this case, overlapping is assumed to happen at the fluid domain level; nevertheless, other solutions involving overlapping of thermal structures may also be considered.

In the case presented, the STH code must provide to the CFD domain the wall temperature and the CFD code transfers the heat flux information to the STH code. Heat flux may be provided in two distinct ways. One may provide it by calculating the heat flux across the coupled surface through the CFD code; in this way consistency between the calculated fluid bulk temperatures in the overlapped domain must be verified. Another approach consists in calculating the heat flux as

$$q''_{CFD} = h_{STH}(T_{w,STH} - T_{f,CFD}) \quad (2)$$

thus requiring that the convective heat transfer coefficient calculated by the STH code and the volume averaged temperature calculated by the CFD code must be taken into account. Consistency between the heat fluxes calculated by the two codes must be checked again in order to assure the energy balance is respected.

Depending on the application, the user may choose for one of the two approaches; however, the more conservative one, ensuring the same transferred heat, is to be preferred.

3.7. Decomposition (Non-Overlapping) approach

Fig. 7 shows two possible schemes for the decomposition approach. Fig. 7 (a) assumes thermal structures being modelled by the CFD code, whilst Fig. 7 (b) instead allocates the thermal structures in the STH domain.

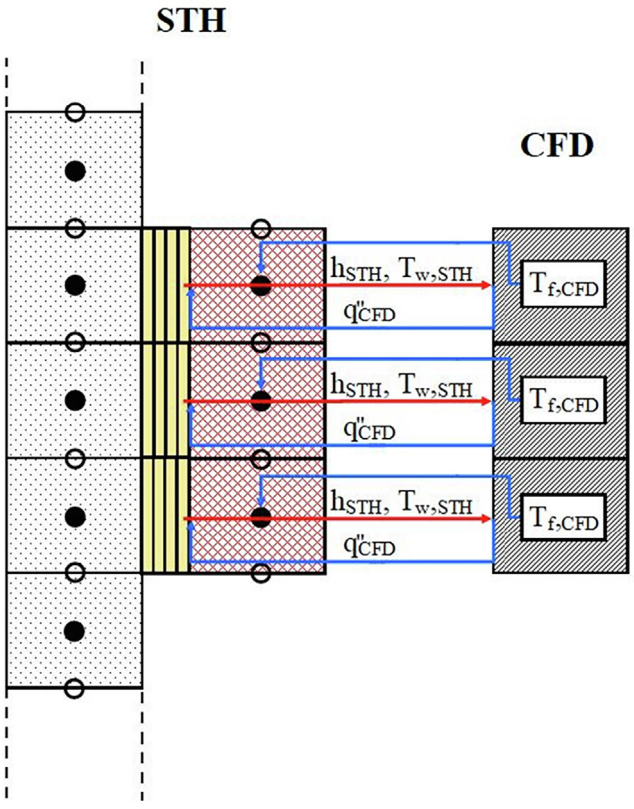

Fig. 6. Thermal Boundaries - Overlapping Approach.

Again, the coupling consists in providing two information: the wall temperature and the heat flux. In case (a) the boundary condition to be imposed to the CFD domain may be assumed of the third kind, i.e. convective heat transfer. Consequently, the STH code must provide the CFD code with the calculated heat transfer coefficient and the bulk temperature of the fluid. CFD in response provides the STH code with the calculated wall temperature. The consistency of the calculated heat flux must be checked in order to assure the fulfilment of the energy balance.

In case (b) instead, thermal structures belong to the STH code. An imposed temperature condition is applied on the CFD wall, in response CFD provides the heat flux to be imposed on the walls of the STH code. As an alternative, CFD may provide the bulk temperature and the convective heat transfer coefficient: nevertheless, these values cannot be always calculated straightforwardly and imposing the heat flux turns out to be a simpler approach. In addition, by directly imposing the heat flux, a better closure of the energy balance is assured. In both cases, the temperature values provided by the STH code may be used as calculated by the STH or interpolated in order to provide the CFD code with improved boundary conditions. Interpolation clearly adds an assumption that cannot be considered reliable for every application, it is again up to the user selecting a discretization refinement which is suitable for the considered application. Depending on the addressed case, the solution reported in Fig. 7 (a) or in Fig. 7 (b) may be preferable; the more conservative in terms of balance equations should be usually selected. Nevertheless, for coupling facing two-phase flow on the STH side, solution 7(a) may be more suitable as it grants higher calculation stability (Galleni et al., 2020). In fact, owing to the intrinsic difficulties in simulating heat transfer involving a two-phase mixture, imposing a heat flux may induce large fluctuations in the calculated heat transfer coefficient wall temperatures and flow patterns; by imposing the wall temperatures, instead, the system turns to be more stable.

4. Time-Advancing numerical schemes: A deeper insight

As anticipated in section 2.6, several time-advancing numerical schemes are available in literature and the user may select the most suitable depending on the addressed application. The numerical schemes may be subdivided into three main groups: explicit, semi-implicit and implicit schemes. Among the semi-implicit schemes, which predict the conditions for the new time-level performing iterative calculations, several proposals exist, some simpler and others more complicated, each one with its own capabilities and downsides. In the following, some of the commonly adopted time-advancing schemes are reported, highlighting their characteristics and suggesting suitable ranges of application.

The same nomenclature adopted by Toti (Toti, 2018) in his work is considered; in particular, U_{CFD} and U_{STH} represent the input vectors for the CFD and STH code respectively, while the output vectors Y_{CFD} and Y_{STH} are instead defined as

$$Y_{CFD} = \Phi_{CFD}(U_{CFD}) \tag{3}$$

$$Y_{STH} = \Phi_{STH}(U_{STH}) \tag{4}$$

where the operator Φ shortly represents all the complex calculation involved during the information processing of both CFD and STH codes.

In general, owing to the sequential nature of the involved calculations, the output data of the CFD domain are used as updated boundary conditions for the STH code and vice versa. Therefore:

$$U_{CFD} = Y_{STH} \tag{5}$$

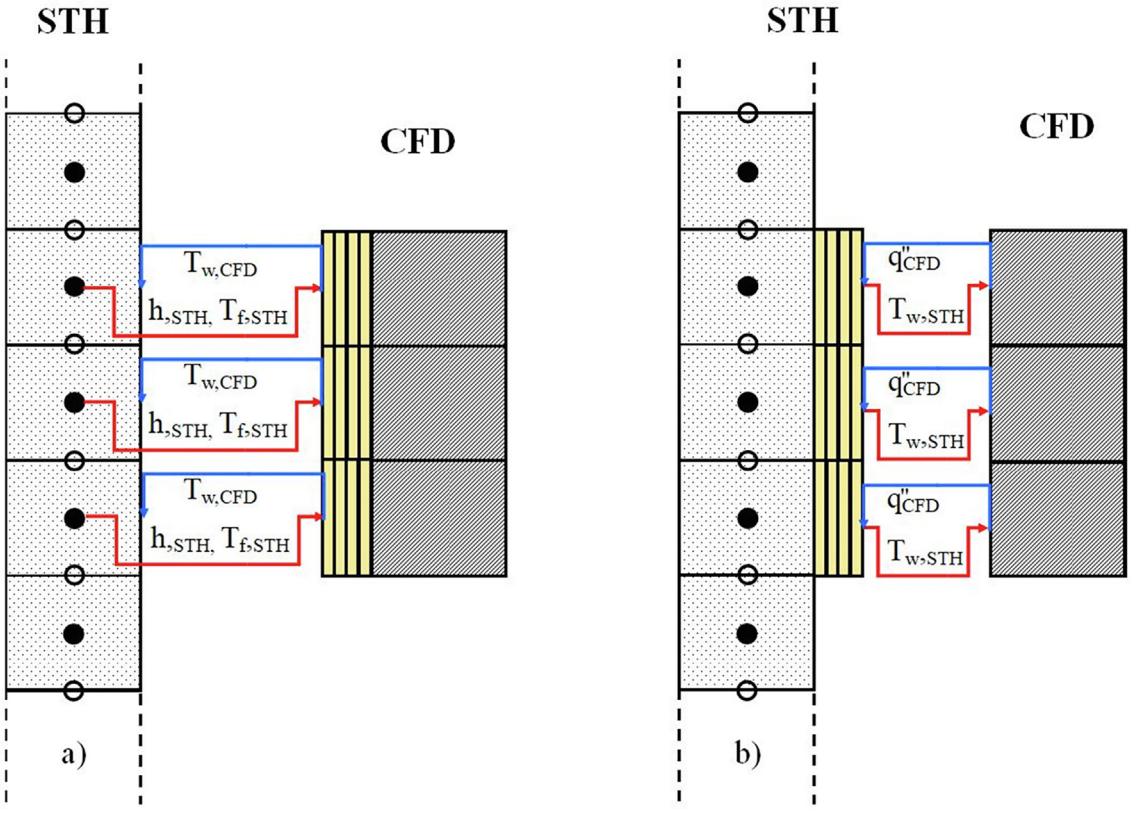

Fig. 7. Decomposition approach schemes with different thermal structures allocation.

$$U_{STH} = Y_{CFD} \tag{6}$$

4.1. Explicit scheme

This is the simplest scheme; it reckons on just a single calculation both for CFD and STH sides for each time step. Fig. 8 shows the calculation phases of the explicit scheme.

As it can be observed, at each new time-step the output data from the STH code are considered as the new input data for the CFD code. The updated boundary conditions are imposed adopting the STH results, while the properties distribution obtained at the previous CFD calculation is maintained as initial condition. After the CFD calculation, the relevant quantities are collected and transferred to the STH code that, with updated boundary conditions, performs its own calculation. The obtained results are then considered as a good estimation of the system behaviour for the current time step and the coupling scheme goes on solving the following one.

This approach does not assure strict fulfilment of the energy, mass and momentum balances at the code interfaces; no check on the consistency of the results provided by the two codes is actually performed. As a consequence, when dealing with fast transients, a very small time-step is required to guarantee a better calculation stability and balance equations closure. Therefore, in order to avoid a large increase of the computational time, this approach is not recommended with respect to the other techniques.

The explicit scheme is instead recommended for simulating transients involving phenomena with low characteristic velocity scales, since this situation allows using longer time-steps without incurring in balancing and stability issues. Though a semi-implicit scheme is, in general, more accurate in terms of balance equation closure, for slow transients it may be worth using the explicit approach since it grants sensibly smaller computational efforts yet maintaining suitable results quality.

4.2. Semi-Implicit schemes

In the present section, some of the most widely adopted semi-implicit schemes are described. In particular, information regarding the fixed-point iteration, the scalar relaxation model and the quasi-Newton method is here reported.

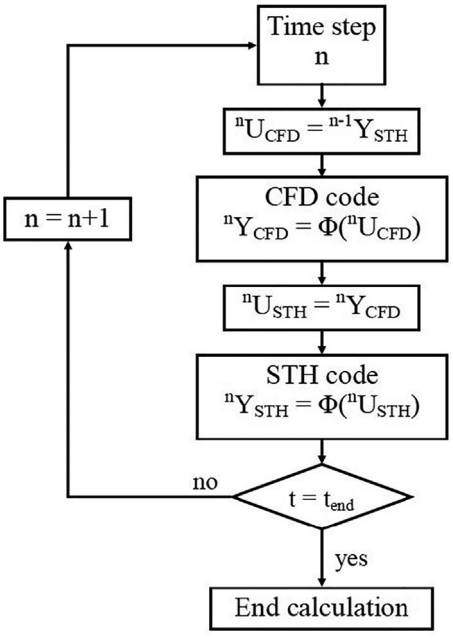

Fig. 8. Explicit Time-advancing scheme flowchart.

4.3. Fixed-point iteration

The fixed-point iteration method is a semi-implicit scheme that performs iterative calculations for each time step until a predefined convergence criterion is fulfilled. This way, the user may define the maximum acceptable error for the energy, momentum and mass balances thus reducing stability issues and allowing adopting larger time-steps than explicit schemes.

Fig. 9 shows the main processes and calculations required for every considered time-step; the parameter n refers to the current time-step, the parameter k, instead, to the current internal iteration. For each time-step and internal iteration, the scheme defines the residual vector. $^{n}R^{k}$ On the basis of the definitions given in relations (3) to (6), the following can be derived:

$$^{n}U^{k}_{CFD} = {}^{n}Y^{k-1}_{STH} \tag{7}$$

$$^{n}U^{k}_{STH} = {}^{n}Y^{k}_{CFD} = \Phi_{CFD}\left(^{n}U^{k}_{CFD}\right) \tag{8}$$

$$^{n}U^{k+1}_{CFD} = {}^{n}Y^{k}_{STH} = \Phi_{STH}\left(^{n}U^{k}_{STH}\right) \tag{9}$$

$$^{n}R^{k} = {}^{n}U^{k+1}_{CFD} - {}^{n}U^{k}_{CFD} \tag{10}$$

Through the analysis of the $^{n}R^{k}$ vector components, or of one of its vectorial norms, the scheme understands if the convergence criterion was achieved or not. If yes, the scheme goes on solving the following time-step, if not another internal iteration k + 1 is performed.

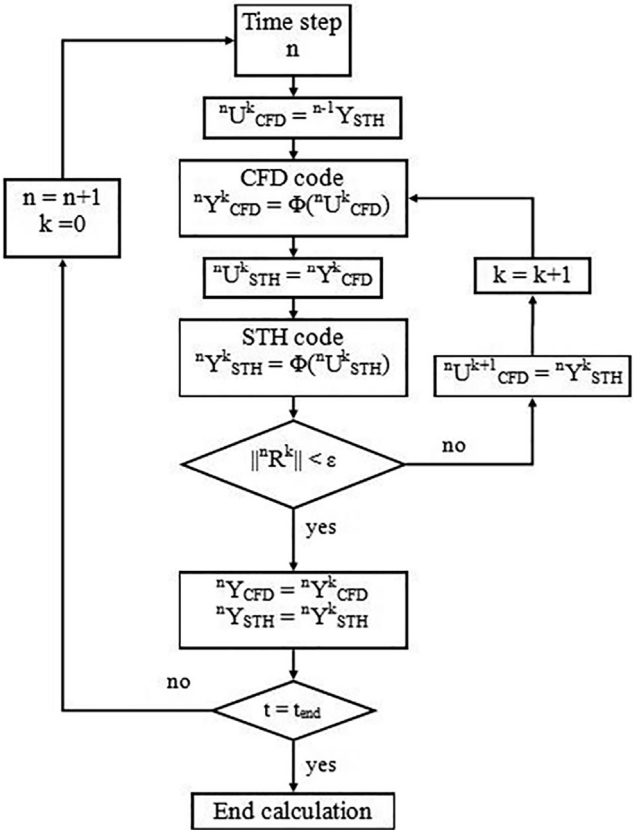

Fig. 9. Fixed-point semi-implicit scheme flowchart.

${}^{n}U_{CFD}^{k+1}$ represents the updated boundary conditions calculated by the STH code to be provided to the CFD code for the next internal iteration while ${}^{n}U_{CFD}^{k}$ represents the boundary conditions that were provided to the CFD code at the beginning of the present internal iteration. If the components of ${}^{n}U_{CFD}^{k+1}$ and ${}^{n}U_{CFD}^{k}$ are sufficiently close, the components of the ${}^{n}R^{k}$ are deemed to be relatively small, thus (normally) evolving towards the fulfilling of the adopted convergence criterion. This means that the predictions of the CFD and STH code are sufficiently consistent to consider the balance equations converged. When the convergence criterion is fulfilled, the results provided by the CFD and STH code during the last internal iteration are promoted to the actual prediction for the present time-step and adopted as initial conditions for the following one.

This scheme is suitable for every application, regardless of the velocity of the involved phenomena. The criterion check performed before proceeding to the next time step allows that consistency between the results calculated by the CFD and STH codes is achieved.

The choice of a suitable convergence criterion is one of the most important settings of the presently considered scheme. Choosing a too large value, the user may lose the capability of reliably fulfilling mass and energy balances while selecting a too small value, the scheme may require unjustifiably large amounts of internal iterations for the calculation of each time-step, thus making vane the gain in computational time due to the adoption of a larger time-step in comparison to explicit schemes.

In some cases, the user is required to introduce an under-relaxation coefficient, to be adopted in the update of ${}^{n}U_{CFD}^{k+1}$, in order to achieve faster convergence or a more robust advancing scheme. In particular, ${}^{n}U_{CFD}^{k+1}$ can be defined as

$$ {}^{n}U_{CFD}^{k+1} = {}^{n}U_{CFD}^{k} + \omega\left({}^{n}Y_{STH}^{k} - {}^{n}U_{CFD}^{k}\right) \tag{11} $$

where ω is the relaxation factor. When facing stability issues, it should be $|\omega|<1$ (under-relaxation), while for achieving faster convergence even values larger than unity (over relaxation) might be considered. Therefore, a generally valid relaxation factor cannot be identified, since it is very case sensitive. In addition, a dynamic definition of the under-relaxation factor may also be considered: the time advancing algorithm may be programmed in order to select suitable values depending on the current time-scale of the observed phenomena, differences in the solution vectors between a time-step and the other, or in the residual vector magnitude.

The definition of a dynamic under-relaxation factor, being suitable for each application, is at the basis of advanced semi-implicit schemes presented in the next sections.

4.4. Scalar relaxation method

As anticipated, being able to define a suitable under-relaxation value for each iteration may significantly accelerate the convergence rate of the adopted method.

In particular, the Aitken Δ^2 (Brezinski and Zaglia, 1991; Küttler and Wall, 2008) must be mentioned. This method improves the capabilities of the fixed-point iteration method in the solution of non-linear equations performing at least one step adopting the secant method. Starting from the fixed-point iteration equation

$$ x^{k+1} = f(x^{k}) \tag{12} $$

it performs a first order Taylor series expansion around the first estimation x_0 assuming the derivative being suitably approximated by a secant. The new estimation is the solution of the following linear system, in which $f(x^1)$, x^1 and $f(x^0)$ are evaluated adopting the fixed-point iteration method.

$$ \begin{cases} y = f(x^0) + \frac{f(x^1)-f(x^0)}{x^1-x^0}(x - x^0) \\ y = x \end{cases} \tag{13} $$

Which leads to:

$$ x^{k+1} = \frac{f(x^1)x^0 - f(x^0)x^1}{\left[f(x^1) - x^1\right] - \left(f(x^0) - x^0\right)} \tag{14} $$

Moving from non-linear equations to the presently considered coupling application, given any internal iteration k^{th} of the n^{th} time step, the previous quantities may be identified as:

$$ x^0 = {}^{n}U_{CFD}^{k-1};\ f(x^0) = {}^{n}Y_{STH}^{k-1};\ x^1 = {}^{n}U_{CFD}^{k};\ f(x^1) = {}^{n}Y_{STH}^{k}; \tag{15} $$

thus leading to the algorithm:

$$ {}^{n}U_{CFD}^{k+1} = \frac{{}^{n}Y_{STH}^{k}\,{}^{n}U_{CFD}^{k-1} - {}^{n}Y_{STH}^{k-1}\,{}^{n}U_{CFD}^{k}}{{}^{n}R^{k} - {}^{n}R^{k-1}} \tag{16} $$

Studying the solution of the linear system of Eq. (11) and Eq. (16), the dynamic relaxation factor may be obtained as:

$$ {}^{n}\omega^{k} = -{}^{n}\omega^{k-1}\frac{{}^{n}R^{k-1}}{{}^{n}R^{k} - {}^{n}R^{k-1}} \tag{17} $$

As it can be noted, two iterations are required in order to obtain the first estimation of ω for the current time step. At the beginning of each time step the relaxation factor may be either arbitrarily assumed equal to a constant or set equal to the one obtained at the end of the previous time-step. For stability reasons, the user may also define a maximum value of the relaxation factor, thus increasing the method robustness.

The presented relation may also be adopted in case of vectors; this may be the case of multiple information transferred between the two codes, such as at a thermal-hydraulic interface.

$$ {}^{n}\omega^{k} = -{}^{n}\omega^{k}\frac{\left({}^{n}R^{k-1}\right)^{T}\left({}^{n}R^{k} - {}^{n}R^{k-1}\right)}{\left|{}^{n}R^{k} - {}^{n}R^{k-1}\right|^{2}} \tag{18} $$

If the components of the vector do not share the same physical variables, being in example a mass flow rate and a temperature, the user shall implement the algorithm adopting dimensionless residuals in order to increase its efficiency. The residual vector may be computed performing a first reference coupling iteration (Toti, 2018).

This method allows obtaining higher convergence rates at a cost of an additional computational effort for each time step. The user shall evaluate the advantages of adopting a more complicated numerical method depending on the addressed application; if only slow transients are expected, the simpler fixed-point iteration method shall be adopted.

4.5. Quasi-Newton method

The Quasi-Newton method is based on a first order Taylor series expansion of the residual vector around the current solution, assuming the higher order terms negligible. This assumption generates the following relation:

$$ {}^{n}R^{k+1} = {}^{n}R^{k} + {}^{n}J^{k}\left({}^{n}R^{k}\right){}^{n}\Delta U_{CFD}^{k} \tag{19} $$

where ${}^{n}J^{k}\left({}^{n}R^{k}\right)$ is the Jacobian matrix containing the partial derivatives of the residual vector components with respect to all the components of the input vector U_{CFD}^{k}, which collects the boundary conditions imposed to the CFD domain. In general:

$$ {}^{n}J^{k}\left({}^{n}R^{k}\right) = \begin{bmatrix} {}^{n}\frac{\partial r_1}{\partial u_1}^{k} & \cdots & {}^{n}\frac{\partial r_1}{\partial u_n}^{k} \\ \vdots & \ddots & \vdots \\ {}^{n}\frac{\partial r_n}{\partial u_1}^{k} & \cdots & {}^{n}\frac{\partial r_n}{\partial u_n}^{k} \end{bmatrix} \quad (20) $$

However, it may not be simple evaluating all the needed derivatives, considering that the involved operations also include the use of CFD codes. Adopting a generally cost-effective procedure, the user may approximate the given derivatives with finite differences:

$$ {}^{n}\frac{\partial r_1}{\partial u_1}^{k} = \frac{{}^{n}r_i^{k} - {}^{n}r_i^{k-1}}{{}^{n}u_j^{k} - {}^{n}u_j^{k-1}} \quad (21) $$

With the evaluation of the Jacobian matrix, the new ${}^{n}U_{CFD}^{k+1}$ may be estimated, through the calculation of ${}^{n}\Delta U_{CFD}^{k}$.

$$ {}^{n}U_{CFD}^{k+1} = {}^{n}U_{CFD}^{k} + {}^{n}\Delta U_{CFD}^{k} = {}^{n}U_{CFD}^{k} + {}^{n}J^{k}\left({}^{n}R^{k}\right)^{-1} nR^{k} \quad (22) $$

Obviously, the estimation of the Jacobian matrix may require a high computational effort, exponentially increasing with the matrix order. Though its estimation would be always required in order to obtain the most suitable matrix for each time-step, several proposals exist in literature which help in defining a possible strategy for increasing the calculation efficiency. In particular, Toti (Toti, 2018) in his work estimated the Jacobian matrix introducing a small perturbation on a single component of ${}^{n}U_{CFD}^{k+1}$ and evaluating its effect on the residual vector components. The so obtained matrix is maintained until the residual drop target:

$$ \frac{{}^{n}R^{k+1}}{{}^{n}R^{k}} \leqslant 0.1 \quad (23) $$

is fulfilled. Otherwise, the Jacobian matrix is updated considering the new system conditions.

Another possible strategy relies on the reduction of the number of components of both the ${}^{n}U_{CFD}^{k+1}$ and ${}^{n}R^{k}$ vectors. As explained in (Toti, 2018), the boundary conditions, i.e. the components of ${}^{n}U_{CFD}^{k+1}$, sharing some physical similitudes may be condensed in a single parameter. Considering an example taken from nuclear applications, multiple mass flow rates exiting from the reactor upper plenum and heading to the steam generators may be processed as a single equivalent mass flow rate, thus reducing the global computational cost. According to the work of Toti (2018), this method proved superior convergence rates in comparison to all the other ones presented in this paper. However, the user must again balance the advantages of faster convergence and the downside of a significantly higher computational cost per single iteration. If the addressed conditions are relatively simple (e.g. limited number of interfaces between the codes), the fixed-point iteration scheme should be in general preferable.

5. Examples of application to liquid metals facilities

As extensively mentioned in the introduction, during the last years, several examples of STH/CFD coupling applications were made available in literature. Among them, some of the works taking into account data collected in the frame of the E-SCAPE and CIRCE experimental campaigns, addressing scenarios featuring the use of liquid metals, are here reported.

5.1. E-Scape

E-SCAPE (European – Scaled Pool Experiment) is a facility set at the Belgian Nuclear Research Centre SCK•CEN aiming at reproducing the MYRRHA reactor Primary Cooling System at a scale of 1/6. The facility provides experimental results, which could help the designers in improving the comprehension of the phenomena that may occur in the full-scale MYRRHA reactor.

The main characteristics of the E-SCAPE facility, compared to the reference values of MYRRHA are reported in (Van Tichelen and Mirelli, 2017).

The system (simplified layout shown in Fig. 10) consists of the primary vessel, two external LBE circuits, the diathermic oil cooling loops, the filling and draining system with the storage tank and the steel structure for piping and tanks.

The power is provided in the main heat source, represented by the active core and the core by-pass region) equipped with electric heaters, providing a maximum power of 100 kW.

The LBE, flowing out of the heater region, enters the barrel region, from which is then directed, through holes in the barrel itself, in the "upper plenum". From here, the coolant enters the external loops, where the heat exchangers and the pumps are located. The LBE is then redirected in the lower plenum, connected to the heaters.

Fig. 11 reports an isometric view of the Primary Cooling System assembly (Van Tichelen and Mirelli, 2017). Scaled replicas of all main components of MYRRHA are present in the main vessel in order to maintain geometric similarity.

The presence of a long piping system, suitable for the simulation by STH codes, together with the upper and lower plena, characterized by 3-D velocity and temperature fields, makes this facility a valuable case study for coupled STH/CFD applications.

Above all, the work by Toti et al. (Toti et al., 2018a, 2018b; Toti, 2018) must be mentioned.

In (Toti et al., 2018), the authors performed pre-test analyses of the behaviour of E-SCAPE both in steady state forced circulation conditions and during a Loss of Flow transient. The decomposition approach was adopted for the spatial discretization of coupling calculations, while a semi-implicit scheme was selected for the time-advancing numerical scheme. Furthermore, the Quasi-Newton method described in 4.2 was adopted. Fig. 12 shows the adopted model highlighting the regions simulated through the STH code RELAP5-3D and the CFD code ANSYS-Fluent. In this first application, CFD was adopted for the analysis of the upper plenum of the experimental facility, while the STH code was adopted both for the lower plenum and all the other pipings (including the heaters region). This choice was made to obtain a better description of the phenomena occurring in the upper plenum which, for its own geometrical shape, induces 3-D temperature and velocity distributions that cannot be accurately modelled via the 1-D approach provided by a STH code. Fig. 13 shows a detail of the adopted CFD nodalization also highlighting the complexity of the addressed region. Fig. 14 shows the boundaries connecting the STH and the CFD domains: six thermal hydraulics boundaries and two thermal boundaries were taken into account. In particular, it must be observed that the two thermal–hydraulic boundaries at the bottom of the upper plenum refer to the channels corresponding to the active part and the bypass region of the heaters, thus allowing taking into account the difference in temperature and mass flow distributions induced by the considered experimental conditions in the different channels. Eventually, for all the coupling interfaces, the conservative approach consisting in the exchange of mass-flow rates and heat fluxes for the thermal–hydraulic and thermal boundaries respectively was adopted, thus improving the quality of the addressed coupled calculation.

Figs. 15 and 16 show the results obtained in (Toti et al., 2018) for the steady state nominal operating conditions (forced flow, maximum power). It can be observed that both the resulting temperature and velocities distributions are quite complicated and the homogeneous temperature distribution that would be predicted by a STH code cannot be considered accurate.

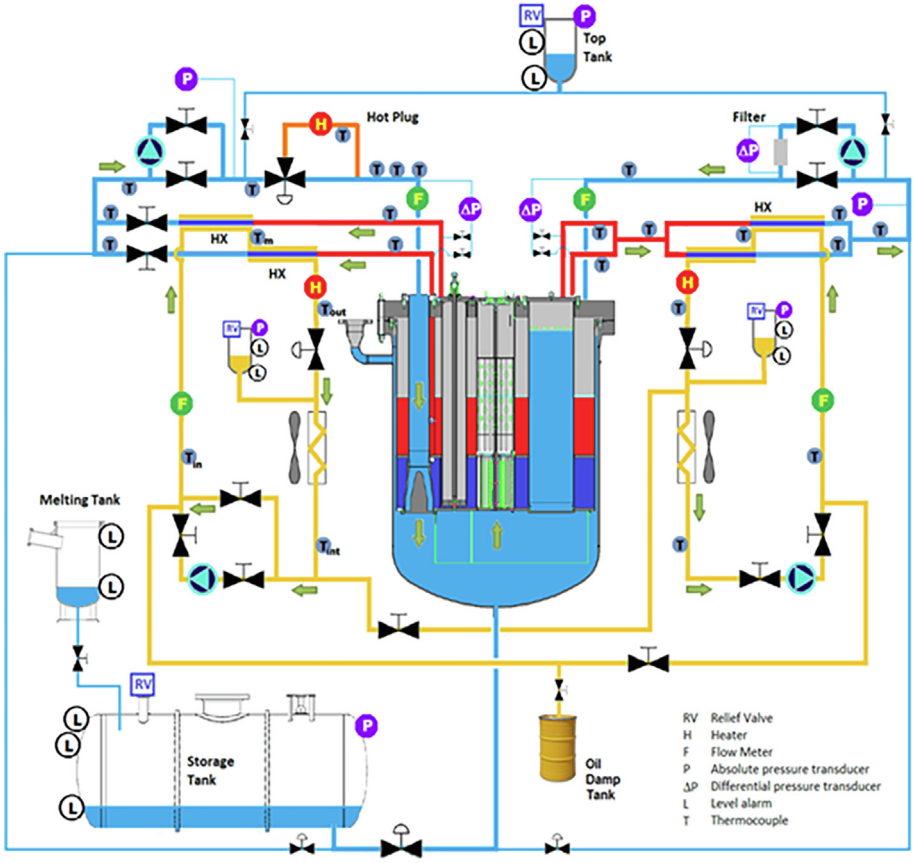

Fig. 10. Simplified layout of the E-SCAPE facility (Van Tichelen and Mirelli, 2017).

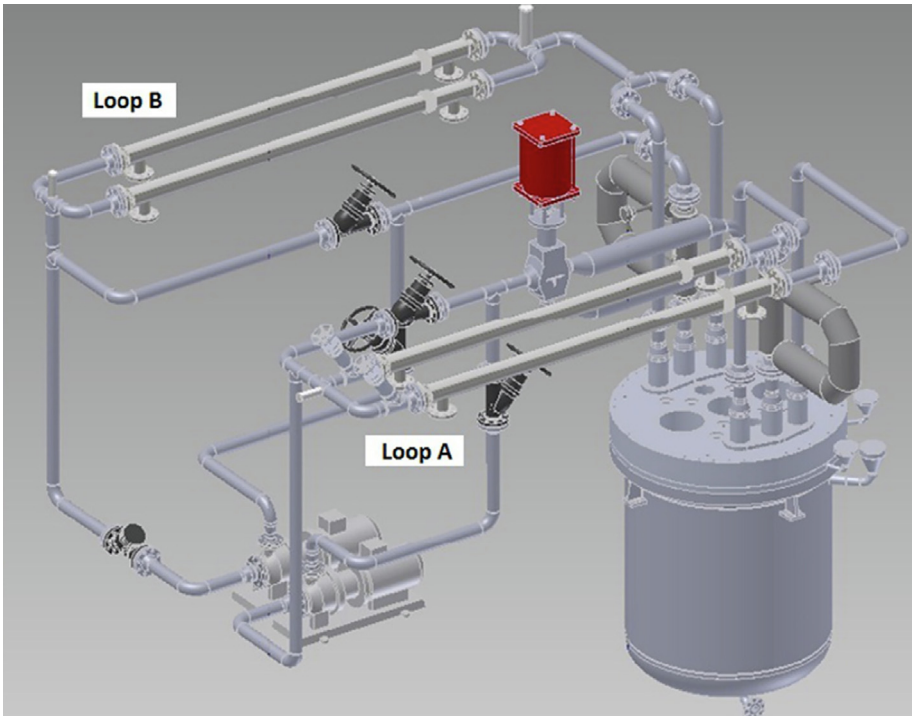

Fig. 11. E-SCAPE Primary Cooling System isometric view (Van Tichelen et al., 2015).

In particular, the hotter regions are located right above the active heaters, in the barrel located in the middle of the upper plenum, while a lower uniform temperature is predicted outside the barrel. This proves that there is a low degree of mixing at the outlet of the heaters region, while the fluid tends to mix outside the barrel. The velocities distribution allows understanding the paths

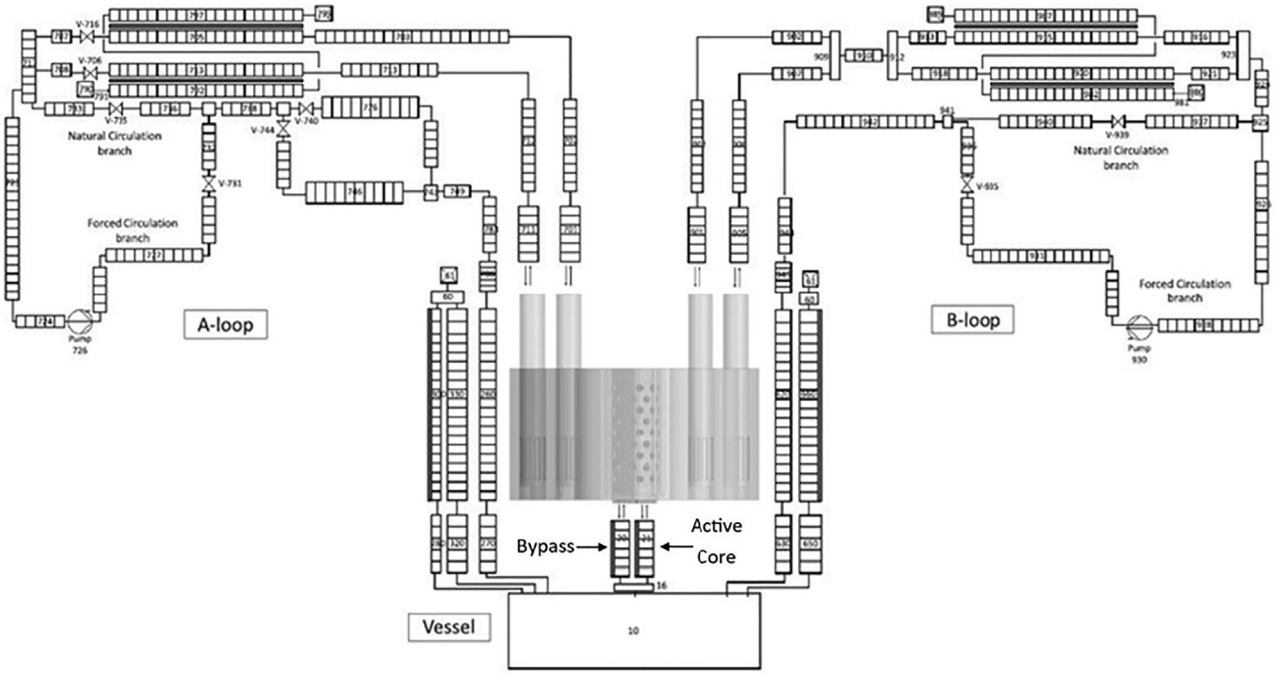

Fig. 12. Coupled model of the E-SCAPE facility (Toti et al., 2018).

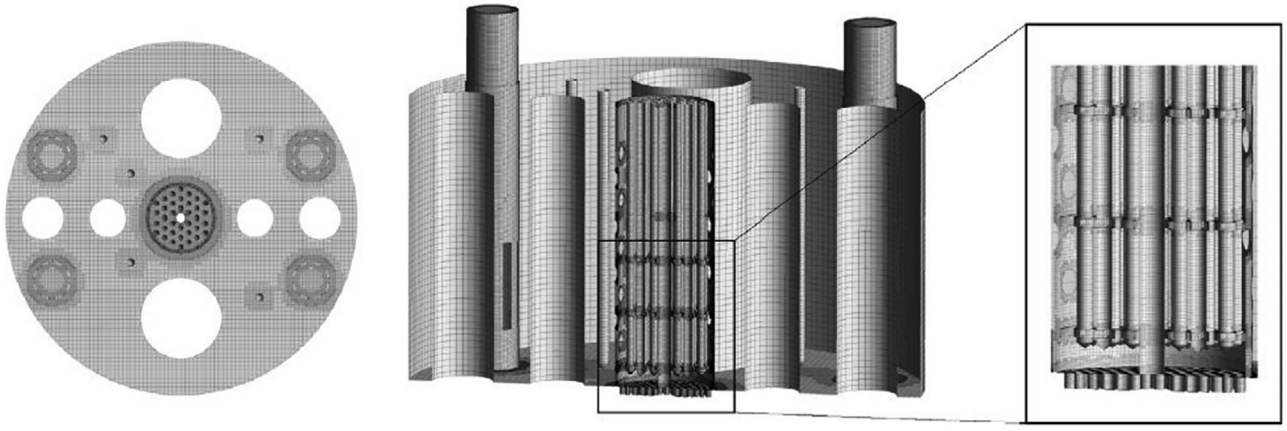

Fig. 13. Details of the CFD computational grid of the upper plenum, figure taken from (Toti et al., 2018).

followed by the fluid which initially moves upwards, towards the free surface, and subsequently spreads inside the pool through the barrel holes. A certain difference in the LBE free surface height between the region inside and outside the barrel was also observed, reporting a higher LBE level in the central region of the barrel. This phenomenon can be explained by two different concurrent reasons: first, the fluid inside the barrel shows a higher temperature and thus a lower density, increasing the level. Moreover, the fluid undergoes a pressure drop when moving through the transversal holes of the barrel towards the upper plenum, which also contribute in increasing the observed free surface distribution difference[1].

Fig. 17 reports, instead, an instantaneous temperature distribution together with velocity vectors for the Loss Of Flow transient case (simultaneous trip of both pumps). Again, it can be observed how the 3-D approach of CFD allows the coupled STH/CFD calculation predicting very peculiar behaviours, such as the radial thermal stratification due to the cold bypass flow rate. In particular, it is worth highlighting the slightly higher mass flow rate passing through the active region predicted by the coupled simulation and the consequently lower bypass mass flow rate (Fig. 18). This behaviour is consistent with the predicted temperature distributions in the Above Core Structure (ACS) predicted by the CFD: the hot plume generated by the active region induces a lighter column of fluid above it, thus reducing the pressure head at the core outlet section. As a consequence, the available pressure drop across the core gets larger thus coherently implying an increase of the mass flow rate.

As Figs. 19 and 20 clearly show, the consequences of the differences between a homogenous temperature and a radially-stratified temperature in the ACS are relevant when considering the outlet temperature time trends; the temperature in the bypass region significantly increases in reverse flow for the STH stand-alone application, because the assumption of

[1] Being the cover gas above the fluid level at constant pressure, the pressure drop across the barrel holes is translated in loss of hydraulic head and reflected in the free surface level difference.

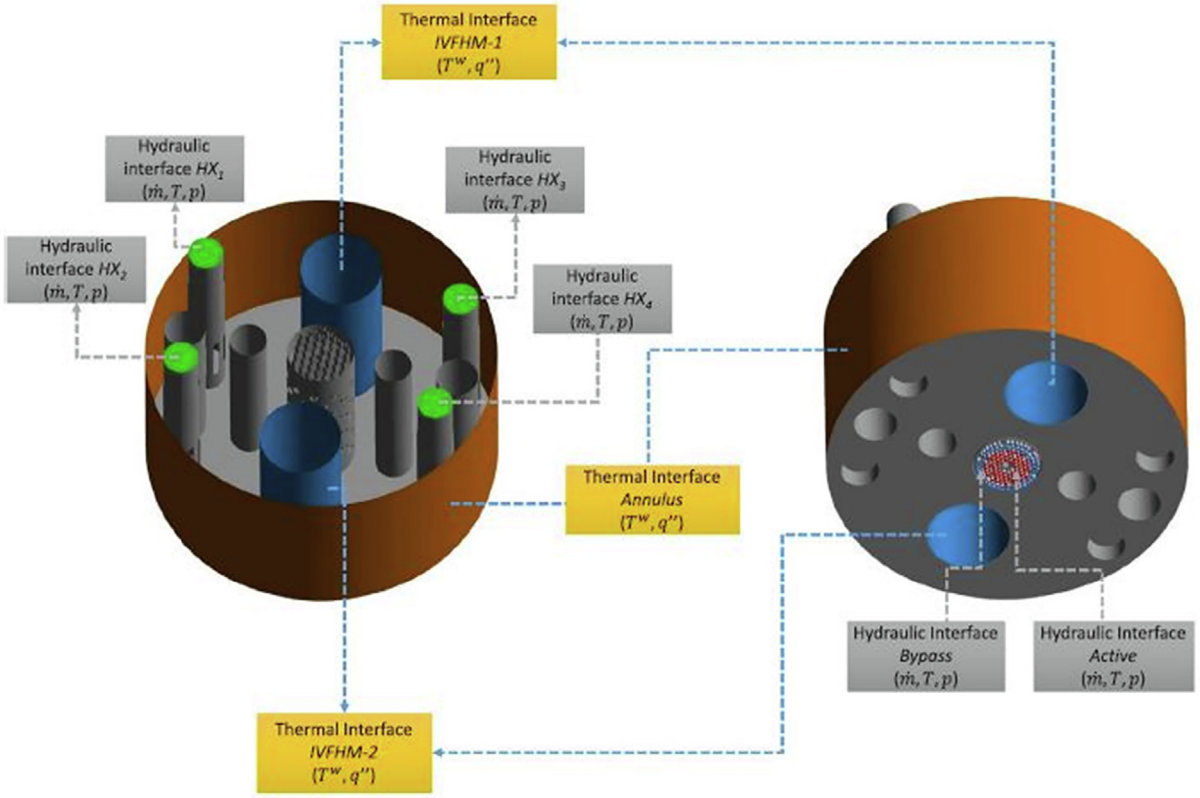

Fig. 14. Location of thermal–hydraulic and thermal boundaries (Toti et al., 2018).

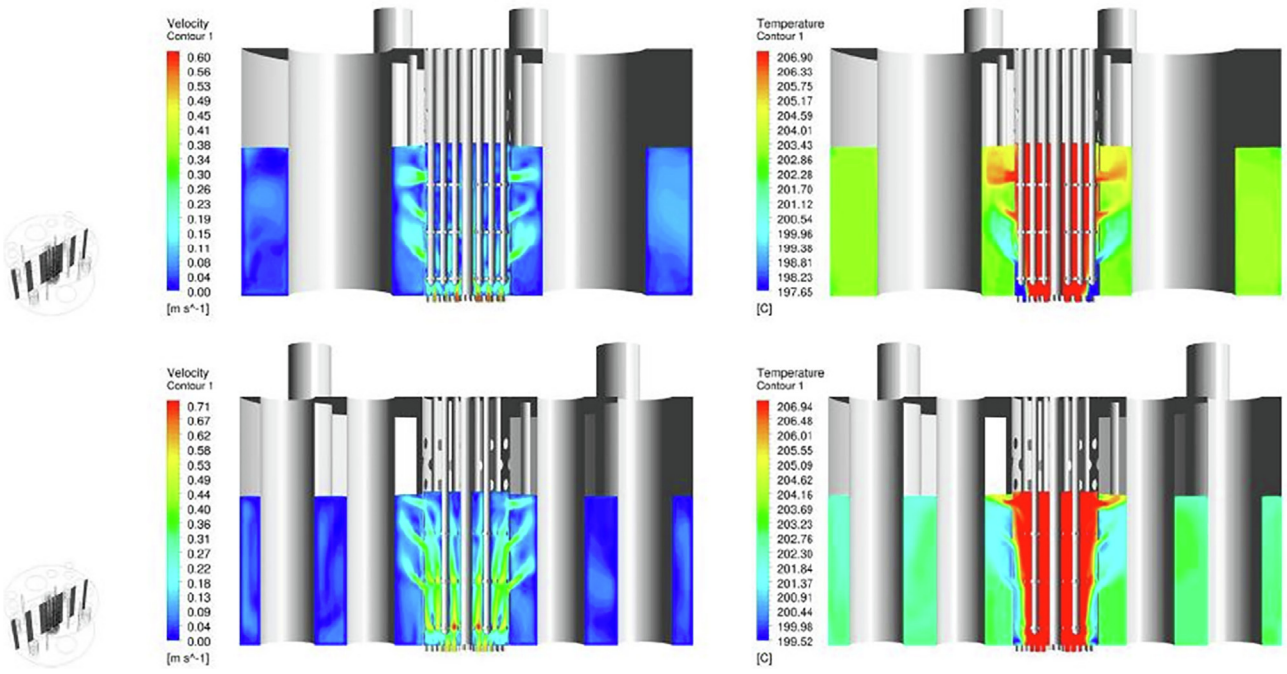

Fig. 15. Upper plenum temperature and velocity distribution for two selected vertical sections (Toti et al., 2018).

perfectly homogeneous temperature in the ACS performed by the stand-alone STH code provides a higher temperature compared to the coupled simulation prediction at the exit of the bypass channel.

At the very beginning of the LOF transient, the mass flow rate is temporarily reversed in the heaters channels (Fig. 18): this is due to the sudden disappearance of the pumps' head causing the pressure drop through the barrel holes to consistently reduce and the free surface levels to equalize[2]. After the flow reversal phase, in the heaters region a larger mass flow rate is predicted by the coupled

[2] In the by-pass channels the flow reversal effect continues for ~400 s because of recirculation phenomena due to the lack of power not generating any driving force.

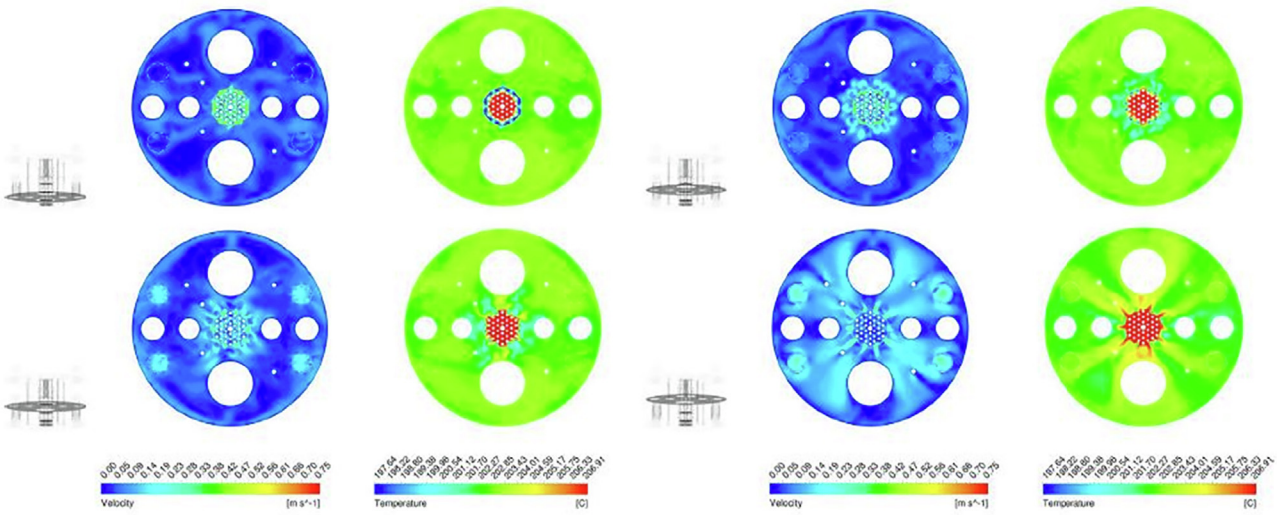

Fig. 16. Upper plenum temperature and velocity distribution for four selected horizontal sections (Toti et al., 2018).

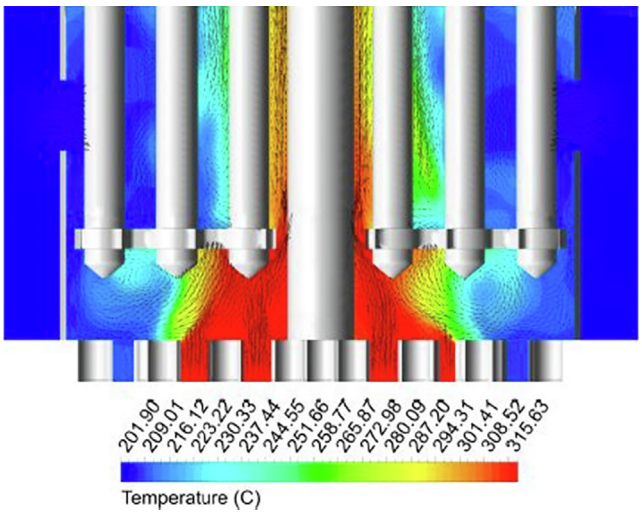

Fig. 17. Temperature contour and vectors velocity in the above core structure at t = 300 s of the LOF transient (Toti et al., 2018).

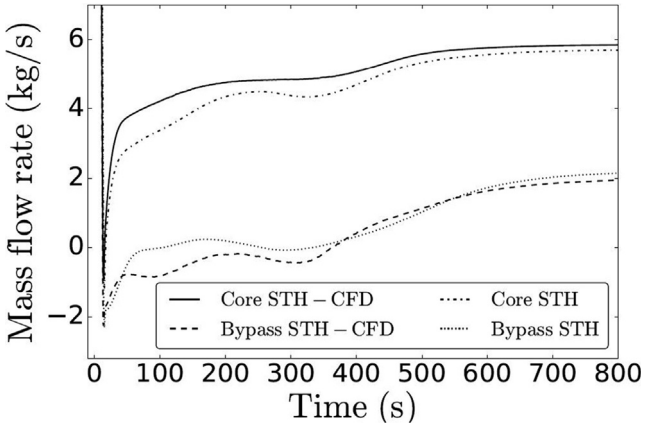

Fig. 18. Mass flow rate in the active and bypass region of the heaters during a LOF transient (Toti et al., 2018).

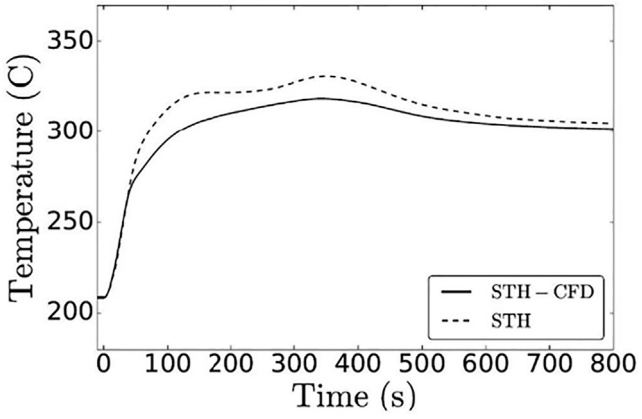

Fig. 19. Heaters active region outlet temperature during a LOF transient (Toti et al., 2018).

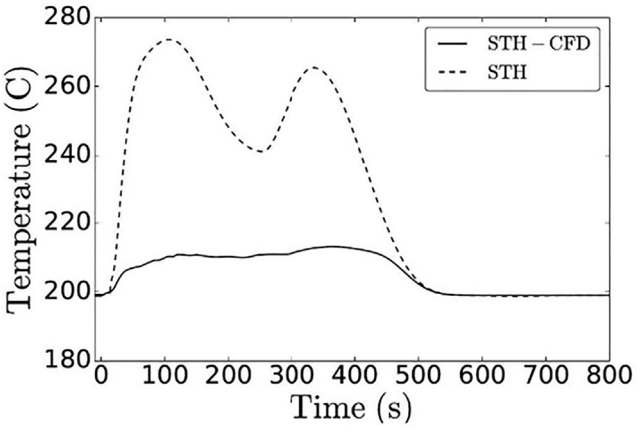

Fig. 20. Heater bypass region outlet temperature during a LOF transient (Toti et al., 2018).

simulations, thus coherently leading to a reduced temperature increase across the heated region.

Eventually, as reported in Fig. 21, adopting a coupled approach allows also predicting stratification phenomena, something that cannot be easily achieved with STH codes because of lack of

thermal conduction within the fluid, thus providing much deeper information and understanding of the involved thermal–hydraulic phenomena in the 3-D plenum.

5.2. Circe

The CIRCE (CIR Culation Eutectic) pool is a facility set at the ENEA Brasimone research centre designed in support to the development of pool type Gen IV LMFRs. The pool hosts an internal loop consisting in several components simulating the primary loop of the reactor itself (Figs. 22 and 23). Again, the presence of a loop immersed in a 3-D environment (the pool) makes this facility a valuable benchmark for the application and validation of coupled STH/CFD techniques; in particular, coupled STH/CFD calculations were recently performed for the latest version of the test loop including the HERO bayonet tube steam generator (Pesetti et al., 2018).

These multi-scale analyses concern pre-test calculations of a PLOFA (Protected Loss Of Flow Accident) simulated in the CIRCE-HERO facility, performed at University of Pisa (Zwijsen et al., 2019). The calculations were performed considering the decomposition approach and simulating the various systems adopting RELAP5/Mod3.3 and ANSYS-Fluent. Fig. 24 shows the considered coupling interfaces; CFD was used for simulating the pool, while the STH code was instead adopted for the analysis of the inner loop. Thermal-hydraulic boundary conditions were imposed at the inlet and outlet sections of the loop, equal pressures were instead imposed at the LBE free surface. Figs. 25 and 26 report some of the obtained results; as it can be observed, the coupled calculation provided results in line with the previous STH stand-alone calculations; the mass flow rate trends were predicted quite well, though discrepancies were instead observed for the temperature distributions.

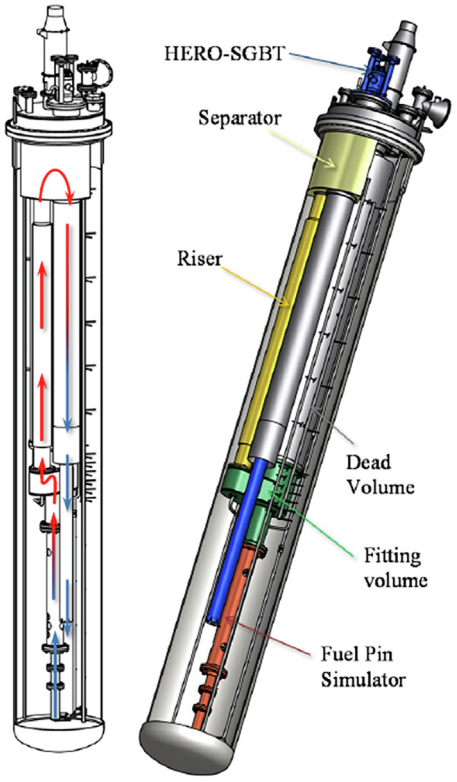

Fig. 22. CIRCE-HERO facility (Pesetti et al., 2018).

It must be here stressed that carrying on a RELAP5 stand-alone calculation of this facility means pushing towards the limits of the STH technique. A realistically representative pool model cannot be

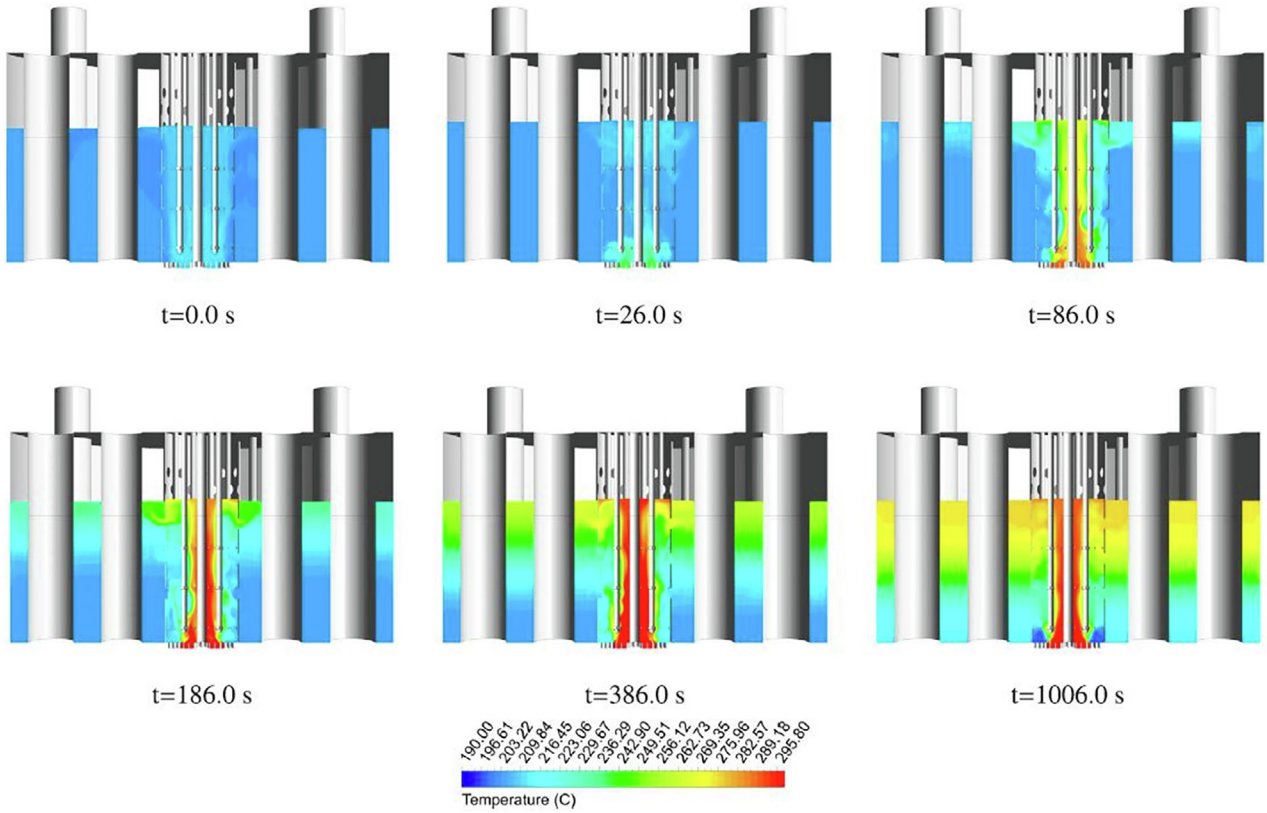

Fig. 21. Upper plenum temperature field evolution for a selected vertical section for the LOF transient (Toti et al., 2018).

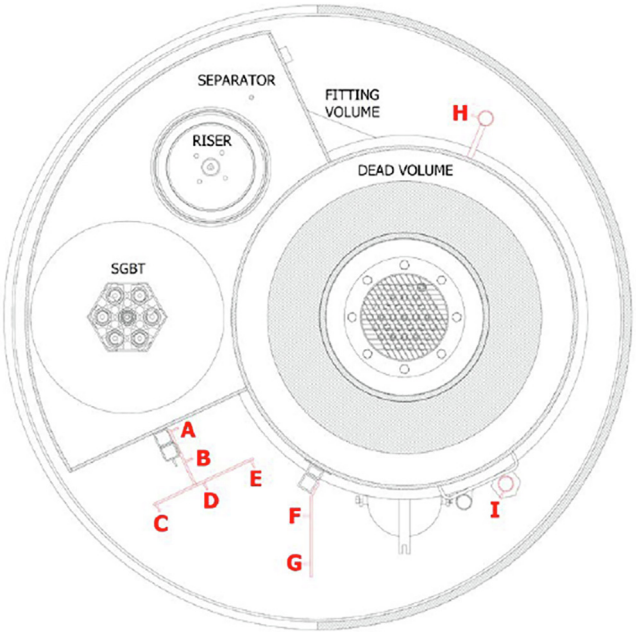

Fig. 23. Radial section of the CIRCE facility and thermocouples positions (Pesetti et al., 2018).

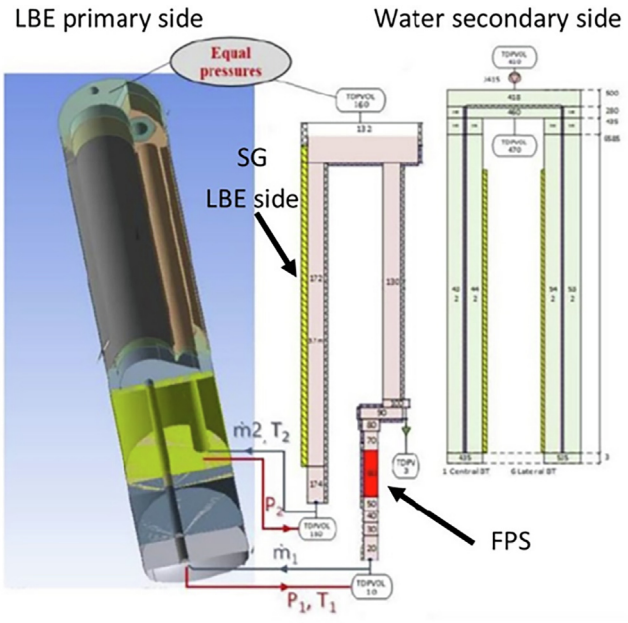

Fig. 24. CIRCE-HERO computational domain for coupled calculations and coupling scheme (Zwijsen et al., 2019).

achieved by relying only on STH codes, and the referred results were obtained after a careful design of the hydraulic components simulating the pool and a tuning process of different model parameters (e.g. pressure drop coefficients) in order to reach a good match of the experimental data. The present RELAP5 stand-alone application must then be considered as a reference for the typical 1-D approach, now progressively replaced by the coupled STH/CFD, more representative. Recently, UniPi published further works involving CFD calculations of the CIRCE pool (Buzzi et al., 2020) and the Fuel Pin Simulator (Buzzi et al., 2020) with the aim to obtain a better understanding of the involved phenomena. In particular, the recirculation phenomena occurring in the lower dome of the pool

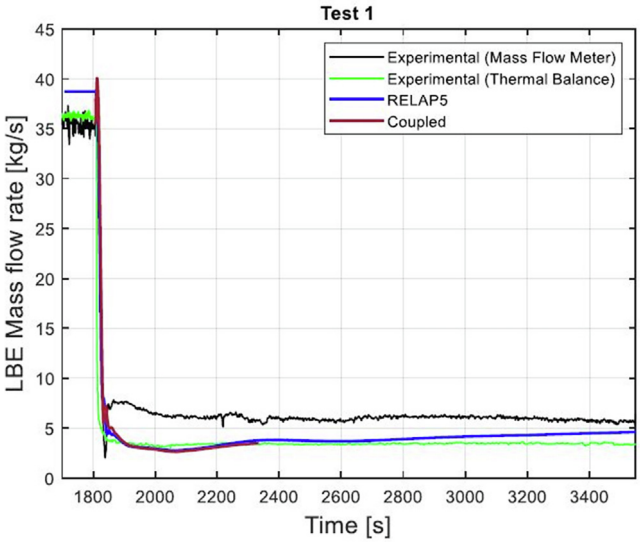

Fig. 25. Mass flow rate in the test section (UniPi) (Zwijsen et al., 2019).

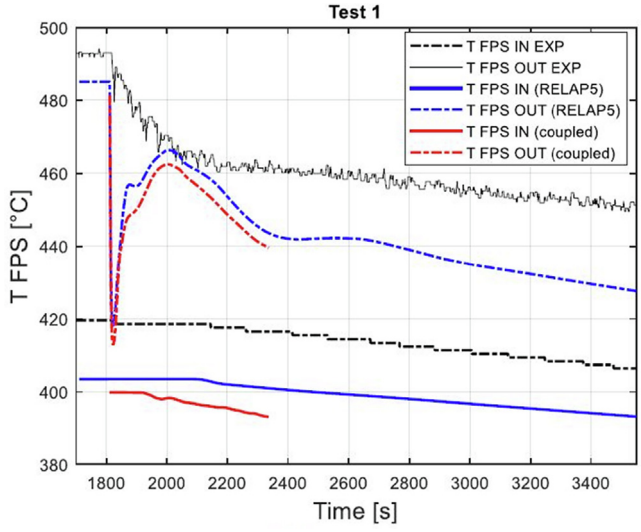

Fig. 26. Temperature profiles at the inlet/outlet of the FPS (UniPi) (Zwijsen et al., 2019).

and the heat transfer occurring between the pool and the Fuel Pin Simulator were deeply analysed thus providing room for a better setting of both the RELAP5 stand-alone and the coupled STH/CFD applications.

The real added value of the coupled calculation relies instead in the velocity and temperature distributions inside the pool region which are provided by the CFD code. As it can be observed from Fig. 27, three distinct temperature regions exist in the pool: a colder one at the bottom, a hotter one at the top and a transition region in correspondence of the Fuel Pin Simulator. In addition, CFD showed that the extension of the cold region is strongly correlated with the predicted velocity fields: in fact, the region where the cold fluid exiting the steam generator recirculates (Fig. 28), perfectly matches the colder (green) region in Fig. 27. In fact, during normal operating conditions, LBE flows out the Steam Generator (SG) at a relatively high velocity, thus implying the impact of the LBE stream against the lower dome of the pool. This in turn generates a large recirculation region before the LBE enters again in the FPS. This phenomenon thus adds some delay between the measured temperatures at the outlet of the SG and at the inlet of

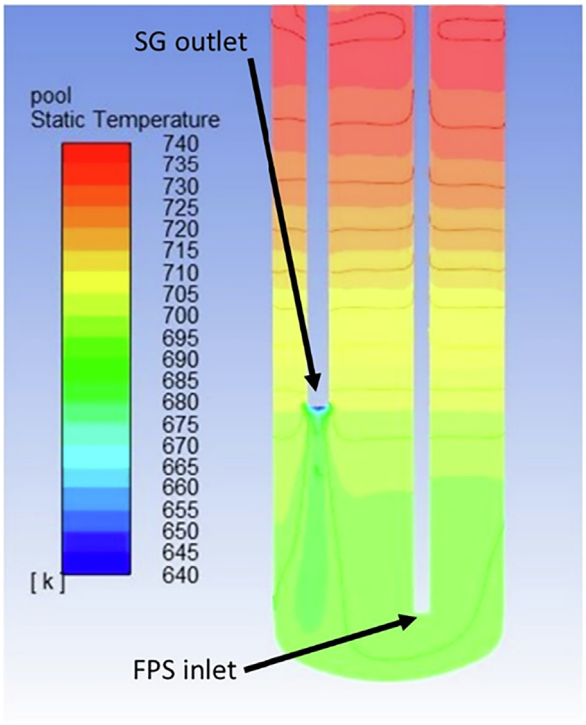

Fig. 27. Temperature distribution inside the pool (UniPi) (Pucciarelli et al., 2020).

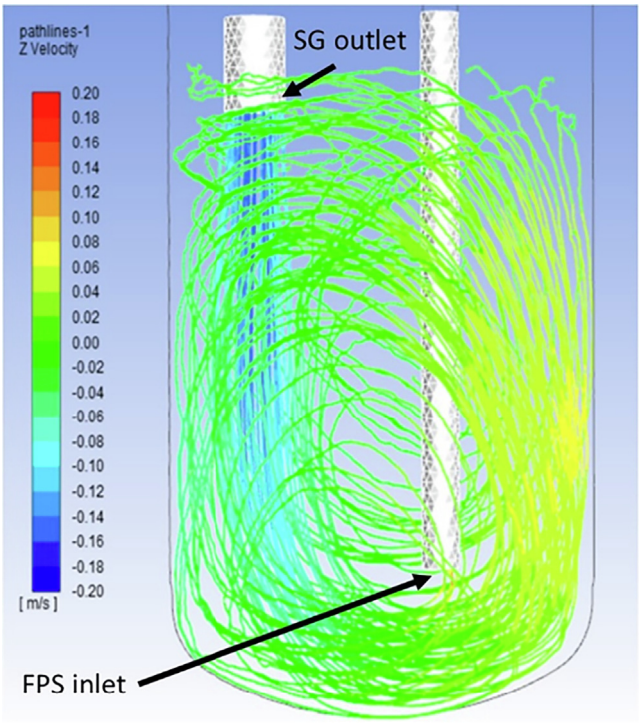

Fig. 28. Velocity streamlines of the lower part of the CIRCE pool (Pucciarelli et al., 2020).

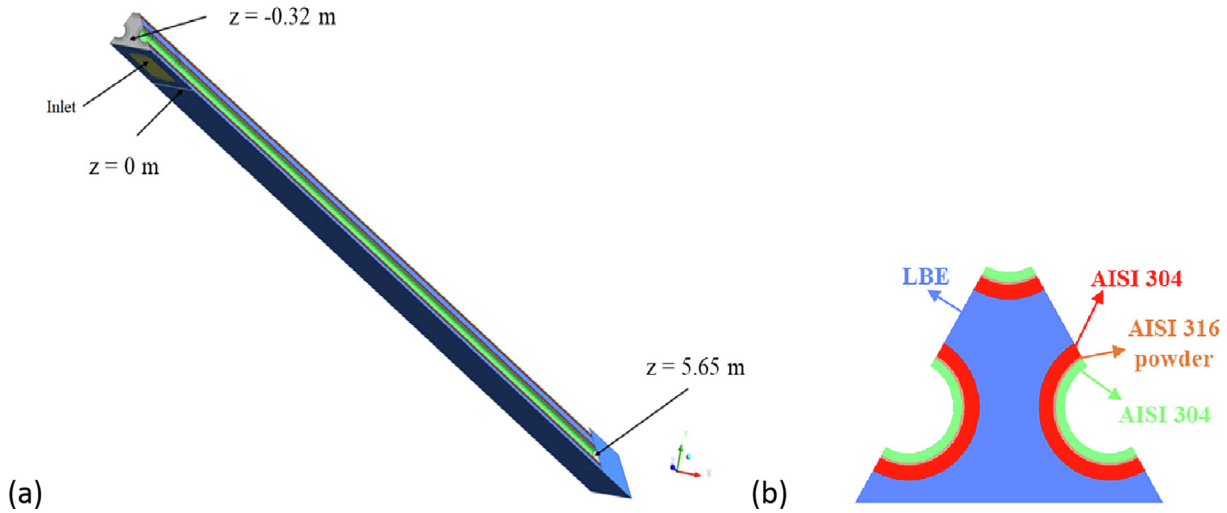

Fig. 29. HERO periodic geometrical CFD domain: overall geometry (a) and material domain (b) (Galleni et al., 2020).

the FPS; this cannot be detected by a STH stand-alone application (where the lower plenum is modelled with a single volume, no temperature distribution is considered and no energy and momentum diffusion is present) and the adoption a coupled application is thus required.

Furthermore, the UniPi developed a pure thermal coupling application in order to simulate the HERO heat exchanger installed in the CIRCE facility (Galleni et al., 2020). In the proposed methodology, the LBE side of the HX-HERO was simulated by the CFD code Fluent (Fig. 29), whereas the secondary side (two-phase flow, water-vapour) was reproduced by RELAP5/Mod3.3; thermal structures allowing heat transfer between primary and secondary loop were included in the RELAP5 domain. The bulk temperature and heat transfer coefficient of the ascending evaporating water obtained from RELAP5 were transmitted to Fluent code; the wall temperature at the water side surface of the pipes was calculated by Fluent and passed to RELAP5 code. In order to exchange data with the system code, 60 artificial surfaces were created on each boundary wall of the CFD domain. At each iteration, wall temperature results from Fluent are averaged over the tubes surface (axially and azimuthally) in each of the 60 above-mentioned zones; then these data are transferred to RELAP5. In turn, RELAP5 gives back 60 data points, which are used to build an axial profile (with linear trend between two consecutive points) of both the two-

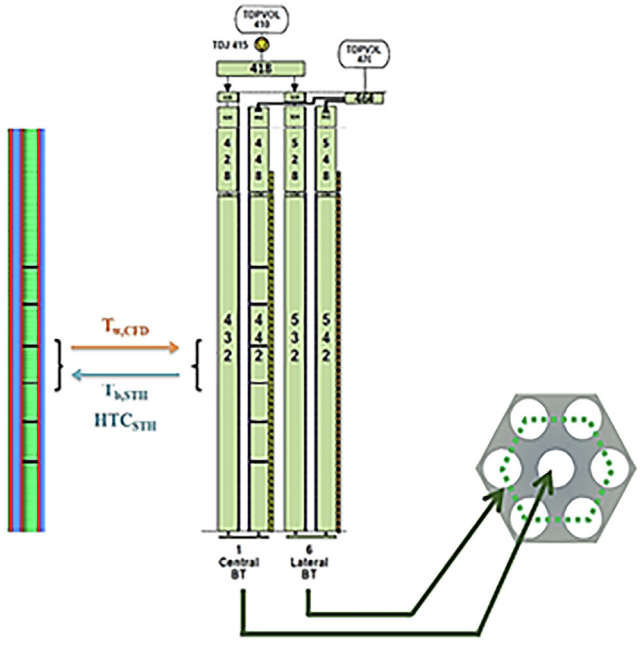

Fig. 30. HERO tubes RELAP5 nodalization and coupling scheme (Galleni et al., 2020).

phase water mixture bulk temperature and the HTC, which then are given to Fluent as boundary conditions. The exchanging scheme is shown in Fig. 30.

The coupling procedure was firstly verified by comparing the obtained results with the analogous ones achieved with the RELAP5 standalone calculation, proving that the developed coupling methodology is reliable. Secondly, the coupled simulations were compared against experimental data. Fig. 31 and Fig. 32 show an example of the results: as it can be seen, the numerical results provide overall a good estimate of the experimental data. In addition, thanks to the CFD contribution, temperature distributions in the rod bundle were obtained, thus relevantly improving the accuracy of the adopted model with respect to the 1-D approach provided by STH codes stand-alone applications. In addition, it must be stressed that the temperature values measured by thermocouples positioned on the SG rods could only be obtained with the adopted coupled STH/CFD approach. In fact, since RELAP5 considers the LBE flow area as a series of volumes characterized by global geometrical parameters (flow area, hydraulic diameter), the simulation cannot appreciate the detail of the different subchannels, thus impairing the quality of the obtained results. The adoption of the coupled simulation also allows the user observing the behaviour of the different water tubes: while in a RELAP5 standalone application the tubes must be considered equivalent, in the coupled calculation one may highlight the obvious differences occurring between the central tube and the six surrounding ones, thus improving the modelling capabilities and the obtained results.

6. Conclusions and future developments

The present work describes general guidelines to be followed when performing coupled STH/CFD calculations simulating operating conditions involving different characteristic time and length scales. This approach allows the user exploiting the best capabilities of both the considered modelling techniques, providing sufficiently reliable predictions with suitable computational efforts.

Some of the most relevant characteristics of the coupling methods were considered and suggestions concerning good practices to be adopted in order to improve the method consistency and stability were provided. In particular, attention has been paid to the different spatial discretisation methods and the numerical schemes. Capabilities and downsides of the various approaches were described, also highlighting possible applicability ranges.

Some examples of Liquid Metals applications were also reported, providing the reader with reference information about the implementation issues and typical expected results quality. Though further verification and validation is needed, the coupled STH/CFD applications proved to be a very promising technique

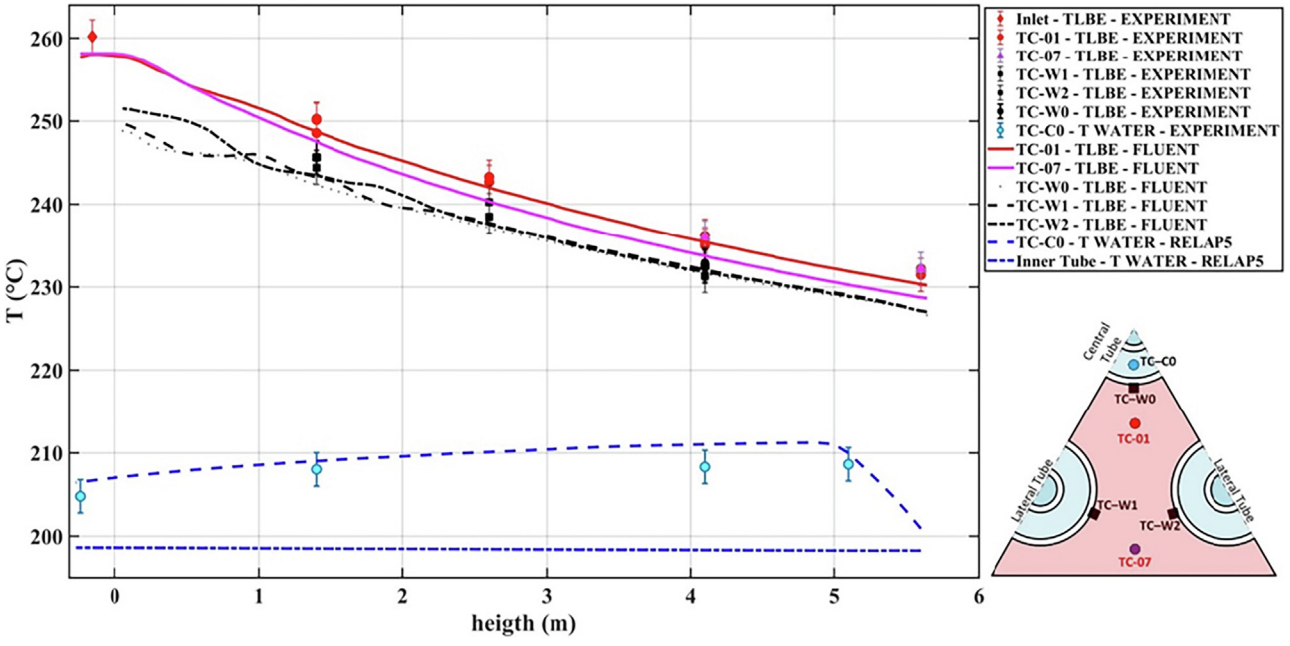

Fig. 31. CIRCE-HERO coupled simulations - Temperature axial evolution in Test 0 (Galleni et al., 2020) Comparison with experimental data.

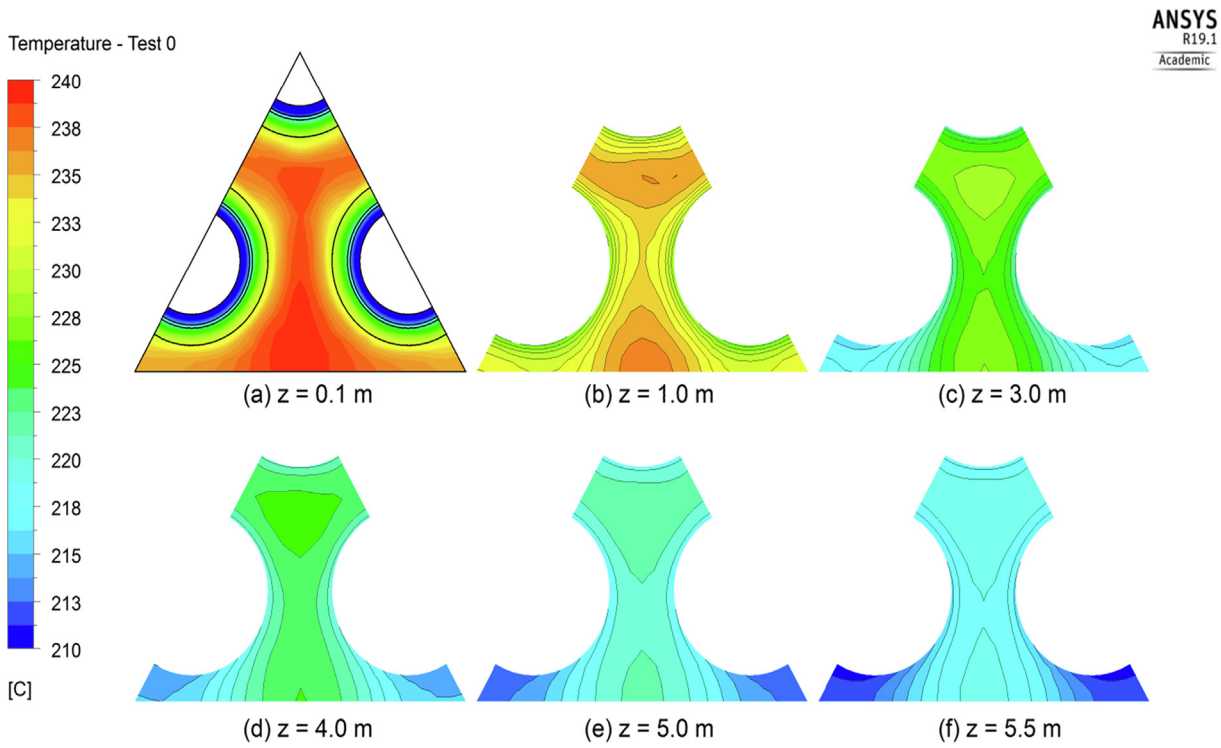

Fig. 32. Coupled simulations - Temperature distribution at different heights - Test 0 (Galleni et al., 2020).

for predicting thermal–hydraulic phenomena in complex systems where 3-D phenomena are relevant.

In the next years, thanks to the continuous improvements in the available computational capabilities, some of the limits of the coupled STH/CFD applications, i.e. the high computational effort required for running long transient CFD calculations, may become less relevant, thus paving the way for a more diffuse use of such modelling techniques. As reported in the present paper, the research community involved in the study, design and licensing of LMRs is really interested in the development of coupled STH/CFD techniques that may overcome the intrinsic limits of 1-D applications; moreover, further works considering coupled codes applications are foreseen in the next future. In the nuclear sector, coupled codes aim at being considered as a recognized and qualified tool for Nuclear Power Plants licensing: this is indeed the real challenge for the future and the development of best practice guidelines, of which this paper may be considered as one of the first steps, is crucial for this achievement.

Declaration of Competing Interest

The authors declare that they have no known competing financial interests or personal relationships that could have appeared to influence the work reported in this paper.

Acknowledgements

This work was performed in the framework of the H2020 MYRTE project. This project has received funding from the Euratom research and training program 2014.2018 under grant agreement No 662186.

References

Aumiller, D.L., Tomlinson, E.T., Bauer, R.C., 2000. A Coupled Relap5 – 3D / Cfd Methodology With a Proof-of-Principle Calculation. Nucl. Eng. Des. 205, 83–90.

Aumiller, D.L., Tomlinson, E.T., Weaver, W.L., 2001. An integrated RELAP5-3D and multiphase CFD code system utilizing a semi-implicit coupling technique. Nucl. Eng. Des. 216 (1–3), 77–87.

INL 2005, "RELAP5-3D Code Manuals revision 2.3 Idaho National Lab, Idaho Falls, ID

ANSYS Inc., 2013. ANSYS Fluent Theory Guide, Release, 15.0

Bertolotto, D., Manera, A., Frey, S., Prasser, H.M., Chawla, R., 2009. Single-phase mixing studies by means of a directly coupled CFD/system-code tool. Ann. Nucl. Energy 36 (3), 310–316.

US NRC, 2007. TRACE V5.0 Theory manual – field equations, solution methods and physical models, US Nuclear Regulatory Commission, Office of Nuclear Regulatory Research

Li, W., Wu, X., Zhang, D., Su, G., Tian, W., Qiu, S., 2014. Preliminary study of coupling CFD code FLUENT and system code RELAP5. Ann. Nucl. Energy 73 (NOVEMBER), 96–107.

Grunloh, T.P., Manera, A., 2016. A novel domain overlapping strategy for the multiscale coupling of CFD with 1D system codes with applications to transient flows. Ann. Nucl. Energy 90, 422–432.

CD-adapco, 2012. USER GUIDE STAR-CCM+ Version 7.04.006.

Park, H.Y. et al., 2010. Coupled fluid dynamics and whole plant simulation of coal combustion in a tangentially-fired boiler. Fuel 89 (8), 2001–2010.

E.ON Engineering. PROATES user's tutorial. PROATES is registered as UKtrademark nos. 1490299 and 1490300; 2007. www.proates.com.

Schuhbauer, C., Angerer, M., Spliethoff, H., Gluger, F., Tschaffon, F., 2014. Coupled simulation of a tangentially hard coal fired 700°C boiler. Fuel 122, 149–163.

APROS Advanced Process Simulation Software, APROS; 2012.

Edge, P.J. et al., 2011. An integrated computational fluid dynamics–process model of natural circulation steam generation in a coal-fired power plant. Comput. Chem. Eng. 35 (12), 2618–2631.

Process Systems Enterprise, gPROMS version 3.2 (2009) http://www.psenterprise.com/gproms.

Hovi, Ville et al., 2017. Integrated transient simulation of a BFB boiler with CFD models for the BFB furnace and dynamic system models for the steam cycle and boiler operation. Energy Procedia 120, 508–515.

AspenTech, 2014. Aspen Plus Help.

Vaquerizo, Luis, Cocero, María José, 2018. CFD–Aspen Plus interconnection method. Improving thermodynamic modeling in computational fluid dynamic simulations. Comput. Chem. Eng. 113, 152–161.

MATLAB. (2018). 9.7.0.1190202 (R2019b). Natick, Massachusetts: The MathWorks Inc.

De Bruyn, D., Abderrahim, H.A., Baeten, P., Leysen, P., 2015. The MYRRHA ADS Project Enters the Front End Engineering Phase. Physics Procedia 66, 75–84.

Toti, A., Vierendeels, J., Belloni, F., 2017ab. Improved numerical algorithm and experimental validation of a system thermal-hydraulic/CFD coupling method for multi-scale transient simulations of pool-type reactors. Ann. Nucl. Energy 103, 36–48.

Van Tichelen, K., Mirelli, F., Greco, M., Viviani, G., 2015. E-SCAPE: A scale facility for liquid-metal, pool-type reactor thermal hydraulic investigation. Nucl. Eng. Des. 290, 65–77.

Toti, A., Vierendeels, J., Belloni, F., 2018aa. Coupled system thermal-hydraulic/CFD analysis of a protected loss of flow transient in the MYRRHA reactor. Ann. Nucl. Energy. 118, 199–211.

Toti, A., Vierendeels, J., Belloni, F., 2018bb. Extension and application on a pool-type test facility of a system thermal-hydraulic/CFD coupling method for transient flow analyses. Nucl. Eng. Des. 331, 83–96.

A. Toti, "Development and Validation of a System Thermal-Hydraulic/ CFD Codes Coupling Methodology for Multi-Scale Transient Simulations of Pool-Type Reactors", PhD Thesis, Ghent University, 2018.

Martelli, D., 2015. Experimental and Numerical Thermal-Hydraulic Analyses in support of GEN-IV Lead-cooled Fast Reactor Design PhD Thesis. University of Pisa.

Angelucci, M., 2018. Coupling between System and CFD codes for the analysis of thermal-hydraulic phenomena relevant for LMFR PhD Thesis. University of Pisa.

M., Angelucci, D., Martelli, G., Barone, I., Di Piazza, N., Forgione, "STH-CFD Codes Coupled Calculations Applied to HLM Loop and Pool Systems, Science and Technology of Nuclear Installations, Volume 2017, Article ID 1936894, 13 pages.

Forgione, N., Angelucci, M., Ulissi, C., Martelli, D., Barone, G., Ciolini, R., Tarantino, M., 2019. "Application of RELAP5/Mod3.3 – Fluent coupling codes to CIRCE-HERO. J. Phys. Conf. Ser. 1224, 012032.

Martelli, D., Forgione, N., Barone, G., Di Piazza, I., 2017. Coupled simulations of the NACIE facility using RELAP5 and ANSYS FLUENT codes. Ann. Nucl. Energy 101, 408–418.

D., Martelli, N., Forgione, G., Barone, A., Del Nevo, I., Di Piazza, M., Tarantino, "Coupled Simulations of Natural and Forced Circulation Tests in NACIE Facility Using RELAP5 and ANSYS Fluent Codes, ICONE22-30552, V004T10A020; 10 pages

M. Jeltsov, K. Kööp, P. Kudinov and W. Villanueva, "Development of a domain overlapping coupling methodology for STH/CFD analysis of heavy liquid metal thermal-hydraulics", NURETH-15, Pisa, Italy, May 12-17, 2013.

G. Barone, D. Martelli, N. Forgione, "Implementation of Lead-Lithium as working fluid in RELAP5/Mod3.3", Fusion Engineering and Design, Volume 146, Part A, September 2019, Pages 1308-1312

Di Piazza, I., Tarantino, M., Agostino, P., Gaggini, P., Polazzi, G., Forgione, N., Martelli, D., 2013. Nacie-UP: an heavy liquid metal loop for mixed convection experiments with instrumented pin bundle. HLMC-2013.

Pesetti, A., Forgione, N., Narcisi, V., Lorusso, P., Giannetti, F., Tarantino, M., Del Nevo, A., 2018. "ENEA CIRCE-HERO Test Facility: Geometry and Instrumentation Description. Report ENEA CI-I-R-343".

Grishchenko, D., Jeltsov, M., Kööp, K., Karbojian, A., Villanueva, W., Kudinov, P., 2015. The TALL-3D facility design and commissioning tests for validation of coupled STH and CFD codes. Nucl. Eng. Des. 290, 144–153.

A. Gerschenfeld, S. Li, Y. Gorsse, and R. Lavastre, "Development and Validation of Multi-Scale Thermal-Hydraulics Calculation Schemes for SFR Applications at CEA", International Conference on Fast Reactors and Related Fuel Cycles: Next Generation Nuclear Systems for Sustainable Development (FR17), 2017, 1–10.

Baviere, R. et al., 2012. Status of CATHARE code for sodium cooled fast reactors. Nucl. Eng. Des. 245, 140–152.

A. Conti et al., "Numerical Analysis of Core Thermal-Hydraulics for Sodium-cooled Fast Reactors," in NURETH-16 (2015).

Barthel, V. et al., 2012. Status of TRIO_U code for sodium cooled fast reactors. Nucl. Eng. Des. 242, 307–315.

F. Roelefs, "Thermal Hydraulics Aspects of Liquid Metal Cooled Reactors", Woodheat Publishing, ISBN: 978-0-08-101981-8 (online), 2019.

L. Mengali, M. Lanfredini, F. Moretti, F. D'Auria, "Stato dell'arte sull'accoppiamento fra codici di sistema e di fluidodinamica computazionale. Applicazione generale su sistemi a metallo liquido pesante", CERSE-UNIPI RL 1509/2011, Pisa, 31 July, 2012.

K., Zhang, "The multiscale thermal-hydraulic simulation for nuclear reactors: A classification of the coupling approaches and a review of the coupled codes" International Journal of Energy Research, 2'2': 44:3295-3315. DOI: 10.1002/er5111

Aulisa, E., Bnà, S., Bornia, G., 2018. A monolithic ALE Newton-Hrylov solver with Multigrid-Richardson-Schwarz preconditioning for incompressible Fluid-Structure Interaction. Computer and Fluids 174, 213–228.

Langer, U., Yang, H., 2018. Numerical simulation of fluid-structure interaction problems with hyperelastic models: A monolithic approach. Math. Comput. Simul 145, 186–208.

Galleni, F., Barone, G., Martelli, D., Pucciarelli, A., Lorusso, P., Tarantino, M., Forgione, N., 2020. Simulation of operational conditions of HX-HERO in the CIRCE facility with CFD/STH coupled codes. Nucl. Eng. Des. 361,. https://doi.org/10.1016/j.nucengdes.2020.110552 110552.

Brezinski, C., Zaglia, M.R., 1991. Extrapolation Methods: theory and practice. North Holland.

Küttler, U., Wall, W.A., 2008. Fixed-point fluid-structure interaction solvers with dynamic relaxation. Comput. Mech 43, 61–72.

K. Van Tichelen, F. Mirelli, "Experimental investigation of steady state flow in the LBE-cooled scaled pool facility E-SCAPE", Proceedings of the 17th International Topical Meeting on Nuclear Reactor Thermal Hydraulics, Xi'an (China), September 3-8 (2017).

Zwijsen, K., Martelli, D., Breijder, P.A., Forgione, N., Roelofs, F., 2019. Multi-scale modelling of the CIRCE-HERO facility. Nucl. Eng. Des. 355.

Buzzi, F., Pucciarelli, A., Galleni, F., Tarantino, M., Forgione, N., 2020. Analysis of thermal stratification phenomena in the CIRCE-HERO facility. Ann. Nucl. Energy 131, 107320.

Buzzi, F., Pucciarelli, A., Galleni, F., Tarantino, M., Forgione, N., 2020. Analysis of the temperature distribution in the pin bundle of the CIRCE facility. Ann. Nucl. Energy 147, 107717.

Pucciarelli, A., Galleni, F., Moscardini, M., Martelli, D., Forgione, N., 2020. STH/CFD coupled simulation of the protected loss of flow accident in the CIRCE-HERO facility. Appl. Sci. 10, 7032. https://doi.org/10.3390/app10207032.

Pucciarelli, A., Galleni, F., Moscardini, M., Martelli, D., Forgione, N., 2020. STH/CFD coupled calculations of postulated transients from mixed to natural circulation conditions in the NACIE-UP facility. Nucl. Eng. Des. 370, (15) 110913.